GENIORS

Research and Innovation Action (RIA)

This project has received funding from the European Union's Horizon 2020 research and innovation programme under grant agreement No 755171.

Start date : 2017-06-01 Duration : 48 Months
http://geniors.eu/

Stability studies of stripping agents

Authors : Mr. Casnati ALESSANDRO (UNIPR), A. Kimberlin, G. Saint-Louis, D. Guillaumont, P. Guilbaud, L. Berthon, A. Casnati, M.C. Gullo; F. Sansone; L. Baldini, T.H. Vu, J.P. Simonin, A. Wilden, D. Schneider, M. Gerdes, G. Modolo, E. Macerata, E. Mossini, M. Mariani, A. Ossola, M. Giola, A. Geist, H. Galan, I. Sánchez, A. Núñez, J. Cobos, S. Bourg

GENIORS - Contract Number: 755171

Project officer: Roger Garbil

Document title	Stability studies of stripping agents
Author(s)	Mr. Casnati ALESSANDRO, A. Kimberlin, G. Saint-Louis, D. Guillaumont, P. Guilbaud, L. Berthon, A. Casnati, M.C. Gullo; F. Sansone; L. Baldini, T.H. Vu, J.P. Simonin, A. Wilden, D. Schneider, M. Gerdes, G. Modolo, E. Macerata, E. Mossini, M. Mariani, A. Ossola, M. Giola, A. Geist, H. Galan, I. Sánchez, A. Núñez, J. Cobos, S. Bourg
Number of pages	45
Document type	Deliverable
Work Package	WP2
Document number	D2.2
Issued by	UNIPR
Date of completion	2019-08-27 17:06:43
Dissemination level	Public

Summary

The present Deliverable collects all the studies carried out, so far, within GENIORS on the Stability of Stripping Agents. The results obtained are collected and divided according to the different type of hydrophilic ligands used. Three main classes of stripping agents were studied: i) sulphonated BT(B)Ps, ii) hydrophilic DGA ligands and iii) PyTri derivatives with focus on PTD.

Approval

Date	By
2019-08-27 17:12:07	Dr. Hitos GALAN (CIEMAT)
2019-08-28 08:29:06	Mr. Andreas GEIST (KIT)
2019-08-28 09:19:26	Mr. Stéphane BOURG (CEA)

CONTENT

This project has received funding from the EURATOM research and training programme 2014-2018 under grant agreement No 755171. The content of this deliverable reflects only the author's view. The European Commission is not responsible for any use that may be made of the information it contains.

This project has received funding from the EURATOM research and training programme 2014-2018 under grant agreement No 755171. The content of this deliverable reflects only the author's view. The European Commission is not responsible for any use that may be made of the information it contains.

ABSTRACT

The present Deliverable collects all the studies carried out, so far, within GENIORS on the Stability of Stripping Agents. The results obtained are collected and divided according to the different type of hydrophilic ligands used. Three main classes of stripping agents were studied: i) sulphonated BT(B)Ps, ii) hydrophilic DGA ligands and iii) PyTri derivatives with focus on PTD.

SO_3-Ph-BTP

CIEMAT: H. Galán, I. Sánchez, A. Núñez and J. Cobos

SO_3-Ph-BTP (2,6-bis(5,6-di(sulphophenyl)-1,2,4-triazin-3-yl)pyridine tetrasodium salt, Figure 1 left), a water soluble BTP, is useful for selectively stripping An(III) from an organic phase containing e.g. TODGA (*N*,*N*,*N*′,*N*′-tetraoctyl diglycolamide, Figure 1 right) as extracting agent, loaded with An(III) and Ln(III) [1]. It has been used in several successful spiked and hot GANEX process tests [2,3,4,5] and in a spiked *i*-SANEX process test [6,7].

The first chemical and radiolytic stability studies of SO_3-Ph-BTP were performed during SACSSES project focus on *i*-SANEX process [8,9].

In the first studies, SO_3-Ph-BTP did not show any signs of degradation in contact with up to 3 mol/L HNO_3 over 120 days. However, gamma irradiation higher than 50 kGy had a negative impact on its performance. With increasing doses, the Am(III) distribution ratios increased (Figure 2a), reducing the separation factor along the irradiation process. After 250 kGy, a loss of approx. 90% of the initial SO_3-Ph-BTP concentration was estimated. It was not possible to quantify its remaining concentration after irradiation neither obtaining a good identification of possible degradation compounds, only hypothetical structures based on mass analysis of irradiated samples were identified.

Additionally, it was studied the interaction between γ-irradiated organic and aqueous phases, for both *i*-SANEX and Euro-GANEX solvent formulations. To simulate more realistic conditions from the point of view of dosimetry, organic phases were submitted to 1 MGy and aqueous phase to low doses (50-300 kGy), individually, since it is expected the aqueous phases received a very low dose if they are not recycled [8,10]. Dose rates from 0.03 to 0.2 kGy/h, and from 0.4 to 0.8 kGy/h, for UO_2 and MOX fuel, respectively, have been estimated for SANEX process [11]. From those experiments it was concluded that even if aqueous phase received a low dose, the loss of efficiency could negatively affect to the global behaviour of the system due to the effect of a degraded organic phase.

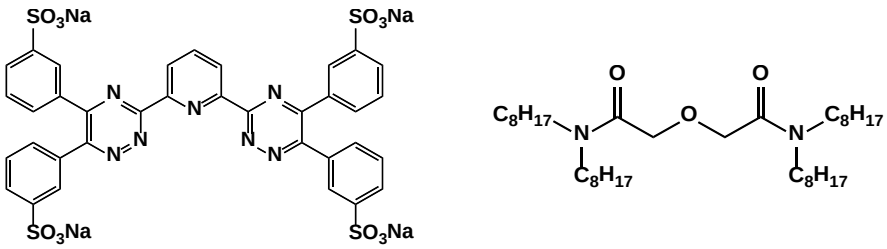

Figure 1. SO_3-Ph-BTP and TODGA structures.

This project has received funding from the EURATOM research and training programme 2014-2018 under grant agreement No 755171. The content of this deliverable reflects only the author's view. The European Commission is not responsible for any use that may be made of the information it contains.

Other way, the *i*-SANEX solvent formulation (consisting of nominally 0.2 M TODGA/5% 1-octanol/dodecane) was γ-irradiated under more realistic conditions from the point of view of a counter-current extraction process in the Idaho National Laboratory radiolysis test loop. In this experiment two phases were submitted to radiation in contact containing both molecules, the extraction and stripping molecules. The results obtained indicated that the performance of the TODGA/SO_3−Ph−BTP system is much better than expected compared with previous radiolysis studies where the diglycolamide TODGA and SO_3−Ph−BTP, had been irradiated separately. In this experiment, the distribution ratios for both metals (americium and europium as analogues of actinides and lanthanides, respectively) were invariant with the absorbed dose, and the separation factors were essentially unchanged to a maximum absorbed dose of 174 kGy (Figure 2b) [12].

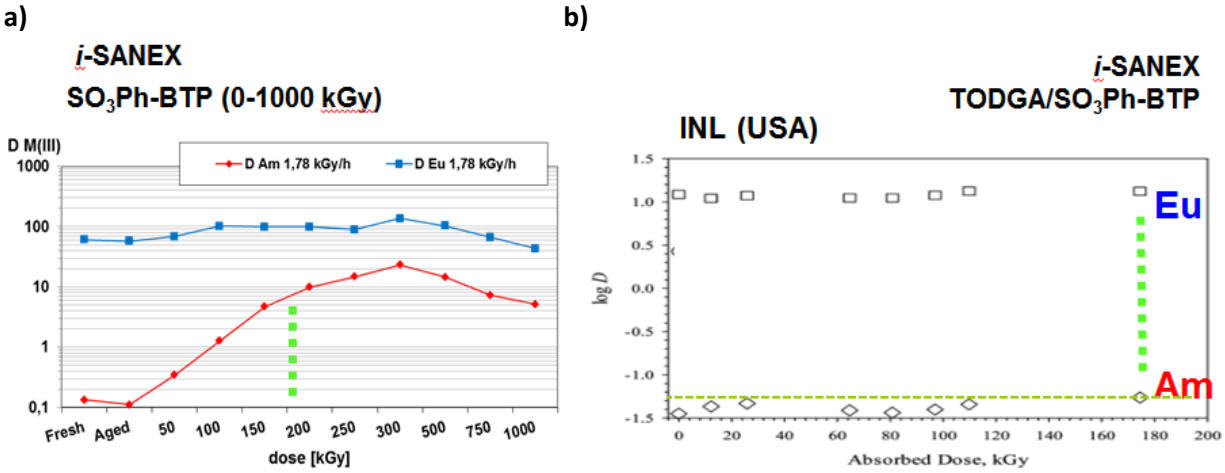

Figure 2. Am(III) and Eu(III) distribution ratios of TODGA/SO_3-Ph-BTP systems as function of dose and irradiation conditions: a) 10 mmol/L SO_3-Ph-BTP in 0.5 mol/L HNO_3 irradiated alone and in static conditions; b) TODGA/SO_3-Ph-BTP systems (18 mmol/L SO_3-Ph-BTP in 0.35 mol/L HNO_3) irradiated under dynamic conditions. Organic: 0.2 mol/L TODGA + 5% 1-octanol in kerosene. Aqueous: SO_3-Ph-BTP + ^{241}Am(III) spiked with ^{152}Eu(III) in HNO_3.

Although, it is not expected that the aqueous phases containing SO_3-Ph-BTP will be recycled, all results point out that to simulate the effects of radiations it is essential to know which are the most relevant process conditions affecting to degradation and long term behaviour. Therefore, further experiments have been carried out during the first years of GENIORS project to gain a better understanding of the radiolytic degradation of SO_3-Ph-BTP and to determinate which are the process relevant conditions should be simulated for estimating the effects of nuclear fuel radiation with easy experiments.

SO_3-Ph-BTP DEGRADATION AS FUNCTION OF PHASES CONTACTED DURING THE IRRADIATION

Comparing previous results for the irradiation of SO_3-Ph-BTP phases individually or in contact with organic phases, but also in static or dynamic conditions, everything point out to a sub-estimation of SO_3-Ph-BTP stability under gamma radiation when aqueous was irradiated individually and in static conditions. These results could be explained due to different reasons, the presence of an organic diluent, the presence of an extractant such as TODGA, the presence more oxygen in dynamic conditions or a combination of all these factors. Therefore, the aim of the stability study was to gain more in-depth knowledge of the factors affecting the degradation of full systems, taking into account the composition of all phases related for i-SANEX or Euro-GANEX processes and the

This project has received funding from the EURATOM research and training programme 2014-2018 under grant agreement No 755171. The content of this deliverable reflects only the author's view. The European Commission is not responsible for any use that may be made of the information it contains.

experimental conditions used. For that, it was studied the stability and behaviour after irradiation SO_3-Ph-BTP when it is part of two systems, TODGA/SO_3-Ph-BTP and TODGA-DMDOHEMA/SO_3-Ph-BTP.

TODGA/SO_3-Ph-BTP SYSTEMS

First of all, it was checked the γ-irradiation effects on SO_3-Ph-BTP in nitric acid solution as function of SO_3-Ph-BTP concentration for a better comparison between the previous static [8] and dynamic [12] experiments. Two experiments have been carried out: in the first of them, 18 mmol SO_3-Ph-BTP was irradiated individually and then contacted with a fresh organic phase containing 0.2 mol/L TODGA in OK. The second experiment, the aqueous phase consisting in 10 mmol SO_3-Ph-BTP after irradiation was contacted with a fresh organic phase containing 0.2 mol/L TODGA + 5% 1-octanol in kerosene. For both experiments, samples were submitted to ^{60}Co radiation up to 200 and 500 kGy at 3.95 kGy/h at Náyade facility. Figure 3 shows Am and Eu distribution ratios obtained for both experiments. As it was observed in the first studies, both aqueous phases loss almost totally the efficiency of An(III)/Ln(III) separation at 200 kGy when aqueous phases are irradiated individually.

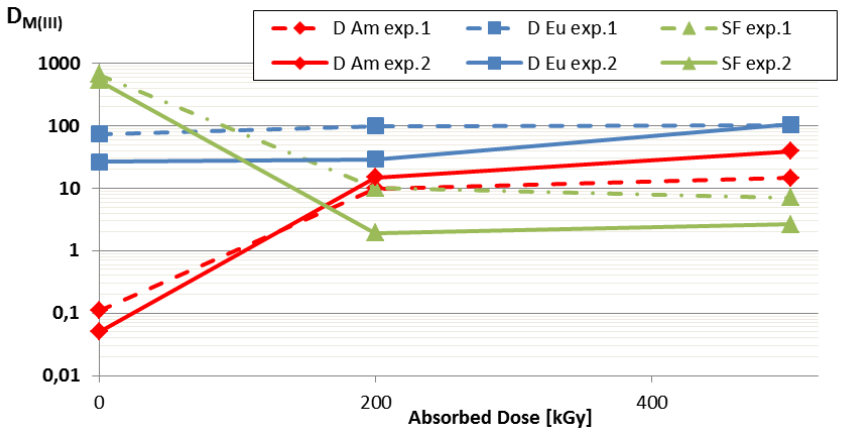

Exp.1: Organic phase fresh, 0.2 mol/L TODGA + 5% 1 octanol in kerosene. Irradiated aqueous phase, 10 mmol/L SO_3-Ph-BTP + ^{241}Am(III)+^{152}Eu(III) in 0.5 mol/L HNO_3.

Exp.2: Organic phase fresh, 0.2 mol/L TODGA in kerosene. Irradiated aqueous phase, 18 mmol/L SO_3-Ph-BTP + ^{241}Am(III)+^{152}Eu(III) in 0.5 mol/L HNO_3.

Figure 3. Am(III) and Eu(III) extraction of fresh and irradiated SO_3-Ph-BTP samples at different doses (200 and 500 kGy).

In parallel to those experiments, to compare the behaviour against γ-irradiation when organic and aqueous phases are irradiated in contact, three different irradiation experiments were carried out. On one hand, it was studied the influence of the contact just with the diluent; and on the other hand, the influence when the diluent contains also an extractant agent. Although the effect on the composition of the organic phase after irradiation is not discussed in this deliverable (see GENIORS HYPAR-1-3_CIEMAT), TODGA irradiated solvent in contact with nitric acid was also included in the experiment as part of a global study. Table 1 shows the composition of the organic and aqueous phases chosen for each experiment and Figure 4 the schematic representation of the different experiments.

This project has received funding from the EURATOM research and training programme 2014-2018 under grant agreement No 755171. The content of this deliverable reflects only the author's view. The European Commission is not responsible for any use that may be made of the information it contains.

It is possible to find on the bibliography many papers highlighting the relevance of the oxygen presence or radicals coming from water radiolysis in the mechanism of degradation [13,14,15]. This could also be also the reason of discordant results obtained for phases irradiated alone or in contact. Therefore, in order to know if these conditions are relevant for simulating the global degradation or not, systems shown in Table 1 were also submitted to radiation in three different ways as (Figure 4): (1) in presence of air, (2) in presence of an inert atmosphere such as argon and (3) using an air sparging flux. The argon atmosphere was chosen to check the system stability in absence of oxygen whilst the air sparging flux simulates a better contact between phases and aerated solution during the irradiation process.

Table 1 Composition of the organic and aqueous phases irradiated in contact and under different experimental conditions.

	Phases	Irradiation experiment		Air	Argon	Sparging
Experiment 1	Org.	TODGA 0.2 M in OK	**IRR**	Exp 1.1	Exp 1.2	Exp 1.3
	Aq.	HNO_3 0.5 M	**IRR**			
Experiment 2	Org.	OK	**IRR**	Exp 2.1	Exp 2.2	Exp 2.3
	Aq.	BTP 0.018 M in HNO_3 0.5 M	**IRR**			
Experiment 3	Org.	TODGA 0.2 M in OK	**IRR**	Exp 3.1	Exp 3.2	Exp 3.3
	Aq.	BTP 0.018 M en HNO_3 0.5 M	**IRR**			

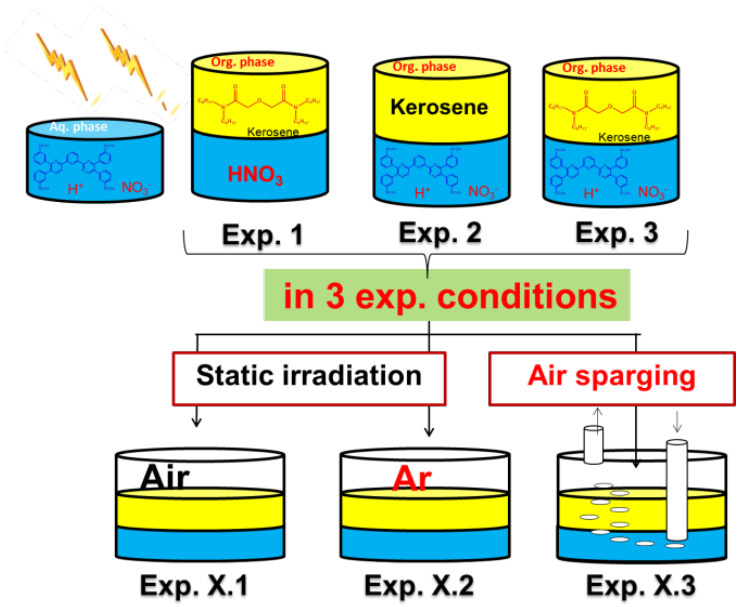

Figure 4. Schematic representation of irradiation performed experiments.

After the irradiation, An(III) and Ln(III) extraction was measured and compared for all solvent compositions and conditions explored. For a real comparison of the extraction experiments and D_M values obtained, the aqueous phases consisting in 0.5 mol/L HNO_3 in Exp 1 were replaced by fresh SO_3-Ph-BTP aqueous phase; and the organic phases consisting in OK in Exp 2 were replaced by fresh TODGA solvent, see Table 2. Then, all Exp 1, Exp 2 and

This project has received funding from the EURATOM research and training programme 2014-2018 under grant agreement No 755171. The content of this deliverable reflects only the author's view. The European Commission is not responsible for any use that may be made of the information it contains.

Exp 3 samples were spiked with ^{241}Am and ^{152}Eu to perform the extraction experiments. Figure 5 and Figure 6 summarise Am and Eu distribution ratios obtained after 200 and 500 kGy for all those experiments.

Table 2. Composition of the organic and aqueous phases: a) during irradiation; b) for comparison of extraction experiments irradiated in contact, up to 200 and 500 kGy.

	Phases	Irradiation experiment		Extraction experiment	
Experiment 1	Org Ph.	TODGA 0.2 M in OK	**IRR**	TODGA 0.2 M in OK	**IRR**
1.1 - 1.2 - 1.3	Aq. Ph	HNO_3 0.5 M	**IRR**	BTP 0.018 M in HNO_3 0.5 M	**FRESH**
Experiment 2	Org Ph.	OK	**IRR**	TODGA 0.2 M in OK	**FRESH**
2.1 - 2.2 - 2.3	Aq. Ph	BTP 0.018 M in HNO_3 0.5 M	**IRR**	BTP 0.018 M in HNO_3 0.5 M	**IRR**
Experiment 3	Org Ph.	TODGA 0.2 M in OK	**IRR**	TODGA 0.2 M in OK	**IRR**
3.1 - 3.2 - 3.3	Aq. Ph	BTP 0.018 M en HNO_3 0.5 M	**IRR**	BTP 0.018 M in HNO_3 0.5 M	**IRR**

For Exp 1 (Figure 5a), as it can be expected, TODGA solvent is moderately degraded after 500 kGy, but it still keeps the extraction, giving place to a slightly reduction of Eu and Am D values. Similar results were observed for the different experimental conditions used (air, argon atmosphere and air sparging).

In Exp 2 (Figure 5b), the system lost the ability to keep An in the aqueous phase after 500 kGy despite of the irradiation of SO_3-Ph-BTP solvent was performed in presence of OK. However, if this result it is compared with results obtained when SO_3-Ph-BTP aqueous phase was irradiated alone (Figure 3, exp 2), D_{Am} increases less after 200 and 500 kGy. Therefore, kerosene seems to provide such a protection over SO_3-Ph-BTP aqueous phase, since An(III) is better kept in the aqueous phase until the same gamma doses. Similar results were also observed for the three different experiment conditions used, air and argon atmosphere as well as aerated solution with air flux sparging (Figure 5).

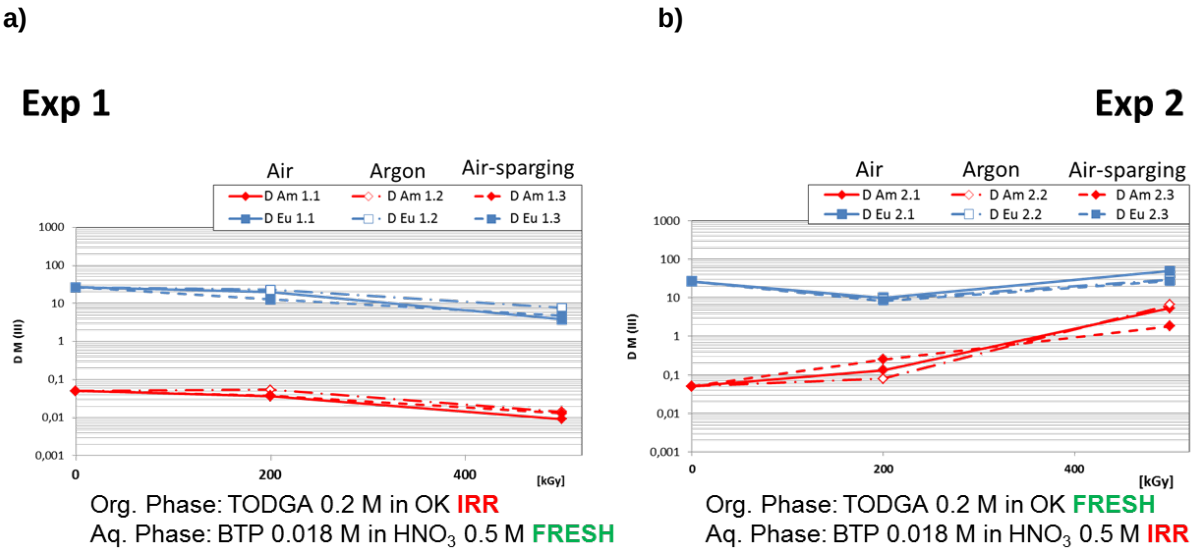

Figure 5. Am(III) and Eu(III) extraction by TODGA / SO_3PhBTP irradiated in different ways. Spiked with ^{241}Am(III) +^{152}Eu(III) (1000 Bq each). Experiments 1 a) and 2 b).

Data obtained for Exp 3 (full system irradiated in contact, TODGA/ SO_3-Ph-BTP) can be seen in Figure 6, and it corroborates that when both phases are irradiated in contact, organic and aqueous, the system keeps better the

This project has received funding from the EURATOM research and training programme 2014-2018 under grant agreement No 755171. The content of this deliverable reflects only the author's view. The European Commission is not responsible for any use that may be made of the information it contains.

performance until higher doses. But also this experiment showed that organic phases containing TODGA seems to provide a better protection on original performance of the system. According to D values obtained, the irradiation of SO_3-Ph-BTP in contact with a TODGA solvent keeps better An in the aqueous phase than when only Kerosene is employed as organic phase.

Exp 3

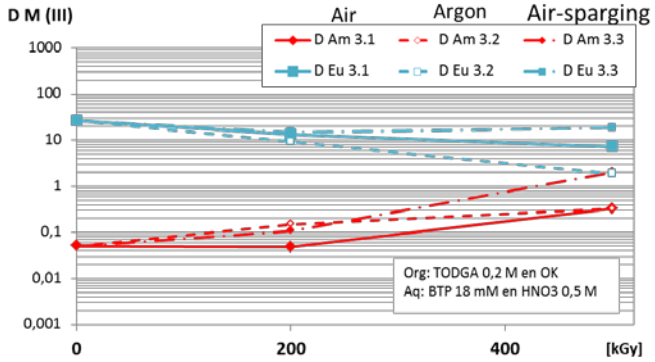

Figure 6. Am(III) and Eu(III) extraction by irradiated TODGA/ SO_3-Ph-BTP systems under different experimental conditions. Aqueous phases were spiked with ^{241}Am(III) +^{152}Eu(III) (1000 Bq each).

All these data pointed out toward the contact between phases is who provides the protection on SO_3-Ph-BTP phase and not the O_2 of the air sparging. Besides, it seems that organic TODGA solvent provided a higher protector effect over SO_3-Ph-BTP phase than kerosene. However, these conclusions should be confirmed with quantitative studies of the remaining SO_3-Ph-BTP concentration.

One of the objectives of this study was also to develop an optimal methodology to analyse the degradation of this molecule by quantifying its remaining concentration after irradiation experiments and to improve the analysis of its possible degradation compounds. Although it was possible to follow three of main mass signals obtained for di, tri and tetra charged compounds by mass spectroscopy (m/z= 214.3, 286.3 and 429.9, respectively, for samples treated with H_2SO_4/H_2O/MeOH), calibrations curves by HPLC-MS were not reproducible. Therefore, assuming that the degradation products do not interfere in the extraction and taking into account the dependency of Am(III) distribution ratios on the concentration of SO_3-Ph-BTP as reported in [16], the decrease in SO_3-Ph-BTP concentration with increasing dose was estimated for the different solvent formulation studied. Figure 7 shows the lineal dependence of D_{Am} as function of SO_3-Ph-BTP concentration in the aqueous phase by the corresponding organic solvent composition, which have been used for estimating the remaining SO_3-Ph-BTP concentration after irradiation experiments (Figure 8).

As it can be seen in Figure 8a (SO_3-Ph-BTP phase irradiated alone), SO_3-Ph-BTP concentration in the aqueous phase is reduced from 18 to 1 mmol after 200 kGy when the aqueous phase is irradiated alone. On the contrary, Figure 8.b shows that after 200 kGy in contact with kerosene the worst results was only a halved reduction of SO_3-Ph-BTP concentration. But also, from Exp 2 (Figure 8b) it can be extracted the highest SO_3-Ph-BTP degradation is produced when air-sparging flux is used and lowest in Ar atmosphere. Therefore, although the contact between phases keeps better the performance along the irradiation, the presence of a higher proportion of oxygen increases degradation of SO_3-Ph-BTP. Otherwise, the pH of the samples could be affected due to the radiolytic degradation as well, and then it could affect to the D values obtained. In Table 3 are summarized the proton concentration for each sample after irradiation. As no relevant changes were observed in pH for Exp 2 neither the TODGA solvent involved had been irradiated, changes in D_{Am} observed in Exp 2 can be only attributed to change in SO_3-Ph-BTP concentration.

This project has received funding from the EURATOM research and training programme 2014-2018 under grant agreement No 755171. The content of this deliverable reflects only the author's view. The European Commission is not responsible for any use that may be made of the information it contains.

To extract conclusion from Exp 3 (Figure 8d) is not simple since in this case both phases, organic and aqueous, are degraded by gamma radiation and changes in D_{Am} (see Figure 6) could not only be attributed to the decrease in SO_3-Ph-BTP concentration, but also to the decrease of TODGA concentration as function of the dose.

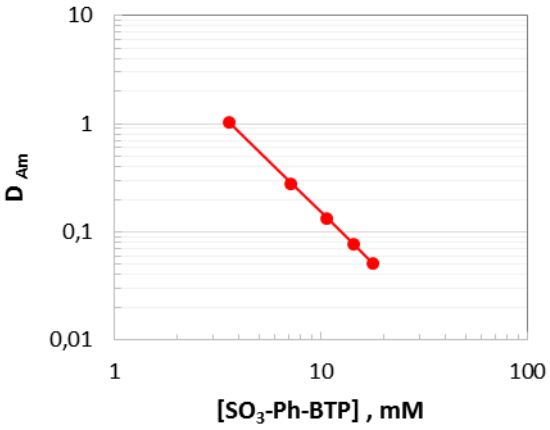

Figure 7. Am(III) distribution ratios of TODGA/SO_3-Ph-BTP system as function of SO_3-Ph-BTP concentration in the aqueous phase. Organic: a) 0.2 mol/L TODGA in OK; Aqueous: 0-18 mmol/L SO_3-Ph-BTP in 0.50 mol/L HNO_3.

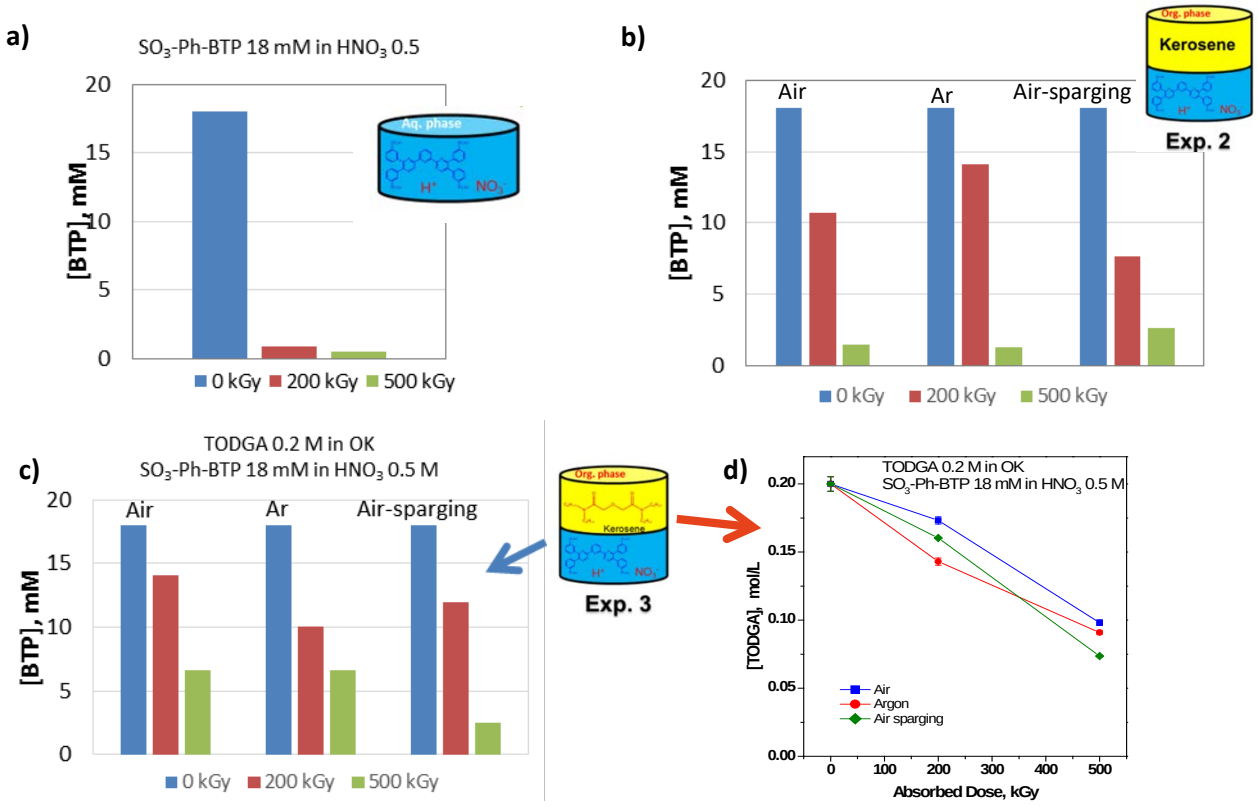

Figure 8. Estimated SO_3-Ph-BTP concentration as function of dose (0-500 kGy), experimental conditions (air and argon atmosphere and using an air flux sparging) and the solvent composition of phases contacted: a) 18 mmol/L SO_3-Ph-BTP in 0.5 mol/L HNO_3 without organic phase; b) 18 mmol/L SO_3-Ph-BTP in 0.5 mol/L HNO_3 + OK; c) 18 mmol/L SO_3-Ph-BTP in 0.5 mol/L HNO_3 + 0.2 mol/L TODGA in OK. d) TODGA concentration as function of dose and experimental conditions.

This project has received funding from the EURATOM research and training programme 2014-2018 under grant agreement No 755171. The content of this deliverable reflects only the author's view. The European Commission is not responsible for any use that may be made of the information it contains.

Table 3. Proton concentrations in the SO_3-Ph-BTP aqueous phase as function of dose and the experimental conditions of experiments.

Sample	$[H^+]$ concentration mol/L		
	0 kGy	200 kGy	500 kGy
SO_3-Ph-BTP_irradiated alone	0.5	0.89	0.98
Ap. Phase of Exp. 2.1	0.5	0.45	0.37
Ap. Phase of Exp. 2.2	0.5	0.45	0.37
Ap. Phase of Exp. 2.3	0.5	0.46	0.58
Ap. Phase of Exp. 3.1	0.5	0.41	0.34
Ap. Phase of Exp. 3.2	0.5	0.37	0.29
Ap. Phase of Exp. 3.3	0.5	0.45	0.47

TODGA-DMDOHEMA/SO_3-Ph-BTP SYSTEM

The water soluble SO_3-Ph-BTP has been also used in several successful spiked and hot EURO-GANEX process tests [17,18,19,20]. The Euro-GANEX solvent consists of a synergic combination of the diglycolamide TODGA (0.2 mol/L) and the malonamide DMDOHEMA [21] (0.5 mol/L) in odorless kerosene. First, this solvent co-extracts lanthanides and actinides from a highly acidic raffinate (HAR); and then, co-stripped all TRU from Ln by using a mixture of water-soluble An complexants; AHA and SO_3-Ph-BTP in 0.5 mol/L HNO_3 (1 mol/L AHA + 0.018 mol/L SO_3-Ph-BTP).

A few studies have been done for the organic solvent of EURO-GANEX system as well as the interaction of organic and aqueous solvents irradiated individually [10,22]. EURO-GANEX organic solvent seems to be very resistant to radiation regarding its Ln/An co-extraction, but it is not really clear is affected the Ln/An separation due to the presence of different TODGA and DMDOHEMA degradation compounds [10]. From the point of view of the aqueous phase, the presence of DMDOHEMA at high concentration in the organic phase of Euro-GANEX solvent could be a positive factor, since according to the previous results, SO_3-Ph-BTP aqueous phase irradiated in contact with TODGA-solvent showed an enhance stability compared to the irradiation in contact with kerosene or the irradiation of the aqueous phase alone. In that sense, similar studies have been carried out for TODGA-DMDOHEMA/SO_3-Ph-BTP and TODGA-DMDOHEMA/AHA-SO_3-Ph-BTP systems.

For that, it was carried out a new irradiation experiment at *Náyade* facility (up to 200 and 500 kGy, at 4.08 kGy/h). Solvent composition of the organic and aqueous phases contacted and submitted to radiation are summarised in Table 4. *System 1* samples correspond to TODGA-DMDOHEMA/SO_3-Ph-BTP studies, and *System 2* samples correspond to TODGA-DMDOHEMA/AHA-SO_3-Ph-BTP studies. Although the effect on the composition of the irradiated organic phase is not discussed here (see GENIORS HYPAR-3_CIEMAT), the irradiated TODGA-DMDOHEMA solvent in contact with nitric acid is also included in the experiment as part of a global study, as it was done in the previous section.

Figure 9 shows fresh and irradiated samples of *Systems 1_2 and 2_2, and Systems 1.3 and 2.3, where* SO_3-Ph-BTP aqueous phases, with or without AHA, have been irradiated in contact with kerosene or TODGA-DMDOHEMA in kerosene. As it can be seen, irradiated aqueous phases containing SO_3-Ph-BTP in presence of AHA show always a darker colour, pointing out to a higher degradation or oxidation of SO_3-Ph-BTP molecule. And when the organic phase contacted was kerosene, third phase formation occurred after irradiation of *System* 1.2 (without AHA), but not after irradiation of *System* 2.2 where AHA is presented.

This project has received funding from the EURATOM research and training programme 2014-2018 under grant agreement No 755171. The content of this deliverable reflects only the author's view. The European Commission is not responsible for any use that may be made of the information it contains.

Table 4. Composition of the organic and aqueous phases (*System* 1 and 2): a) during irradiation up to 200 and 500 kGy; b) in the extraction experiments (Figure 9).

System 1	Phases	Irradiation experiment		Extraction experiment	
System 1_1	Org.	OK TODGA 0.2 M DMDOHEMA 0.5 M	IRR	OK TODGA 0.2 M DMDOHEMA 0.5 M	IRR
	Aq.	HNO_3 0.5 M - -	IRR	HNO_3 0.5 M BTP 0.018 M -	FRESH
System 1_2	Org.	OK - - -	IRR	OK TODGA 0.2 M DMDOHEMA 0.5 M	FRESH
	Aq.	HNO_3 0.5 M BTP 0.018 M -	IRR	HNO_3 0.5 M BTP 0.018 M -	IRR
System 1_3	Org.	OK TODGA 0.2 M DMDOHEMA 0.5 M	IRR	OK TODGA 0.2 M DMDOHEMA 0.5 M	IRR
	Aq.	HNO_3 0.5 M BTP 0.018 M -	IRR	HNO_3 0.5 M BTP 0.018 M -	IRR
System 2	**Phases**	**Irradiation experiment**		**Extraction experiment**	
System 2_1	Org.	OK TODGA 0.2 M DMDOHEMA 0.5 M	IRR	OK TODGA 0.2 M DMDOHEMA 0.5 M	IRR
	Aq.	HNO_3 0.5 M - AHA 1 M	IRR	HNO_3 0.5 M BTP 0.018 M AHA 1 M	FRESH
System 2_2	Org.	OK - -	IRR	OK TODGA 0.2 M DMDOHEMA 0.5 M	FRESH
	Aq.	HNO_3 0.5 M BTP 0.018 M AHA 1 M	IRR	HNO_3 0.5 M BTP 0.018 M AHA 1 M	IRR
System 2_3	Org.	OK TODGA 0.2 M DMDOHEMA 0.5 M	IRR	OK TODGA 0.2 M DMDOHEMA 0.5 M	IRR
	Aq.	HNO_3 0.5 M BTP 0.018 M AHA 1 M	IRR	HNO_3 0.5 M BTP 0.018 M AHA 1 M	IRR

a) *System 1.2 and System 2.2*

Organic: kerosene (OK)
Aqueous: 0.018 mol/L SO_3PhBTP in 0.5 mol/L HNO_3 with and without AHA

b) *System 1.3 and System 2.3*

Organic: 0.2 mol/L TODGA 0.5 mol/L DMDOHEMA in OK
Aqueous: 0.018 mol/L SO_3PhBTP in 0.5 mol/L HNO_3 with and without AHA

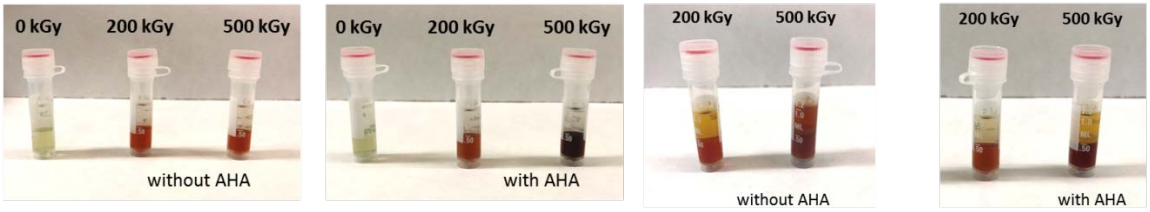

Figure 9. a) Fresh and irradiated aqueous phases of Euro-GANEX system with and without AHA (system 1.2 and 2.2 in Table 4) in contact with kerosene. b) Irradiated Euro-GANEX system, organic + aqueous phases, with and without AHA (system 1.3 and 2.3 in Table 4).

This project has received funding from the EURATOM research and training programme 2014-2018 under grant agreement No 755171. The content of this deliverable reflects only the author's view. The European Commission is not responsible for any use that may be made of the information it contains.

After the irradiation, An(III) and Ln(III) extraction was also measured and compared for all compositions explored. As it was done in the previous experiments, aqueous phases consisting in 0.5 mol/L HNO_3 (with and without AHA) were replaced by the corresponding fresh aqueous phase indicated in green in Table 4; and kerosene of *System* 1_2 and *System* 2_2 were replaced for the organic phase indicated in green in Table 4 (TODGA 0.2 mol/L + DMDOHEMA 0.5 mol/L in OK). Figure 10 and Figure 11 summarise Am and Eu distribution ratios obtained after 200 and 500 kGy for all those experiments.

Figure 10a shows the extraction capacity after irradiation of samples corresponding to *System* 1_1 and *System* 2_1. The important changes observed for Am and Eu distribution ratios are attributed to the presence of AHA in the aqueous phase, since the irradiated organic phase is the same in both experiments. As long as these aqueous phase have not been irradiated, the results should be attributed to the AHA hydrolysis in acid media, which is not discussed here (See TODGA-based solvent degradation deliverables). Figure 10b shows the extraction capacity after irradiation of samples corresponding to *System* 1_2 and *System* 2_2 (SO_3-Ph-BTP and SO_3-Ph-BTP/AHA in nitric acid, which have been irradiated in presence of kerosene). After 200 kGy, the system 1_2 (when SO_3-Ph-BTP is irradiated in contact with OK) shows a significant increase of D_{Am}, which could be explained because TODGA/DMDOHEMA-solvent has a higher Am extraction capacity than TODGA-solvent. Therefore, although the presence of DMDOHEMA in the system could promote also a stabilization of the aqueous phase as it was observed in the previous studies (see Figure 5b), the sum of factors does not provide such as additional stabilization on the global performance of the system. Other way, for the same experiment containing AHA in the aqueous phase (*System* 2.2), a totally different situation was observed, D_{Am} increases slightly as function of dose and but D_{Eu} decreases. The small increases in D_{Am} could be explained by a higher stabilization of SO_3-Ph-BTP in presence of AHA. However, regarding D_{Eu} values, similar results were also observed for *System* 2.1 (Figure 10a), where the aqueous phase used for the extraction was not irradiated. Therefore, factors like AHA hydrolysis in acidic media have to be considered to evaluate these results.

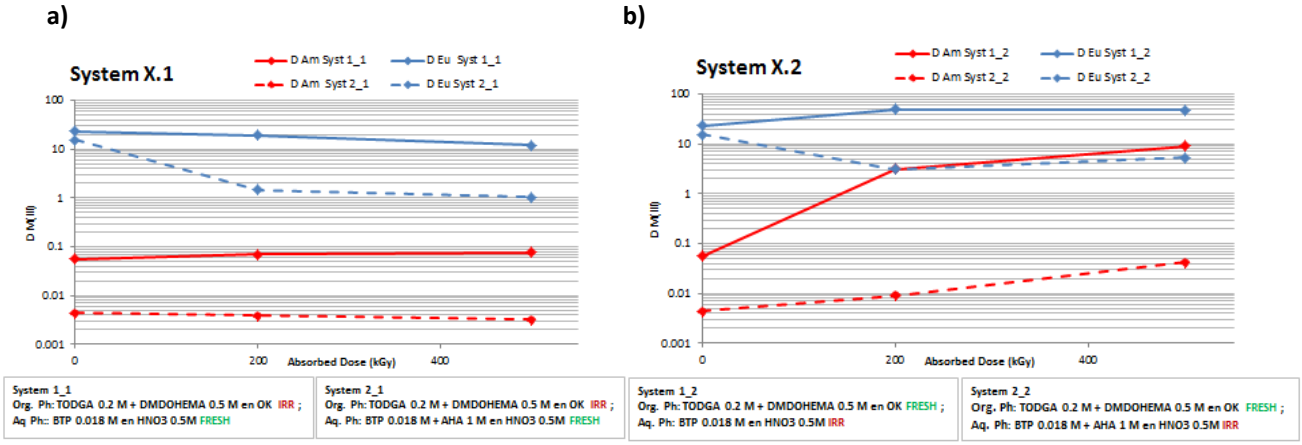

Figure 10. Am(III) and Eu(III) extraction by TODGA-DMDOHEMA/ SO_3PhBTP systems irradiated as it shown Table 4. Spiked with ^{241}Am(III) + ^{152}Eu(III) (1000 Bq each).

Figure 11 shows the extraction capacity after irradiation of samples corresponding to *System* 1_3 and *System* 2_3. In this case, both phases are irradiated together and have not been replaced to perform the extraction experiments, therefore, different factors have to be consider to extract conclusions. *System* 1_3 (TODGA-DMDOHEMA/SO_3-Ph-BTP) shows a similar trend than TODGA/SO_3-Ph-BTP system (see Figure 6). In fact, it can be said that SO_3-Ph-BTP extraction systems keep better performance as function of organic phase in contact during the irradiation experiment as follow: no-organic-phase < OK < TODGA-DMDOHEMA. Once again, the results when AHA is present (*System* 2_3) are similar to previous experiments, *i.e* a slight increase of D_{Am} and a decrease of D_{Eu}. From the point of view of An, the presence of AHA in the system keeps better the performance of the

This project has received funding from the EURATOM research and training programme 2014-2018 under grant agreement No 755171. The content of this deliverable reflects only the author's view. The European Commission is not responsible for any use that may be made of the information it contains.

extraction system. Nevertheless, for a better understanding of all factors involved, quantitative studies of the composition of both phases are needed. Typically, after 200 kGy organic solvents reduce the concentration by ~25% for TODGA and ~20% for DMDOHEMA; and after 500 kGy the degradation increases up to ~50% for TODGA and ~30% for DMDOHEMA (see GENIOR HYPAR-4_CIEMAT). Since, after 200 kGy the reduction in TODGA and DMDOHEMA concentrations is not so important, the effects on SO_3-Ph-BTP stability are easily identified. Therefore, all data obtained until now point out toward it is the contact between phases who provides the protection on SO_3-Ph-BTP phases.

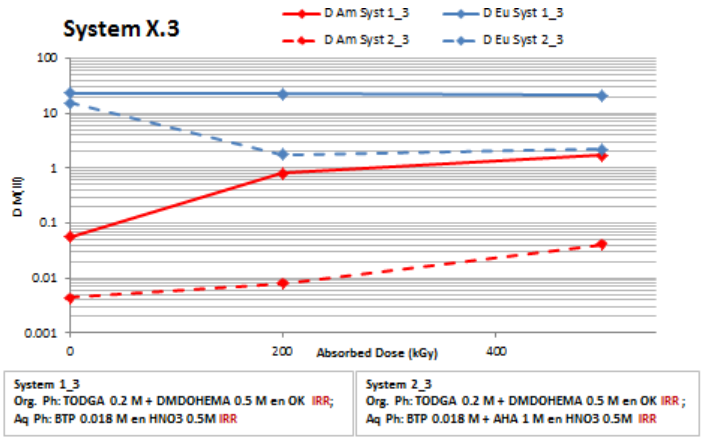

Figure 11. Am(III) and Eu(III) extraction by irradiated TODGA-DMDOHEMA/ SO_3-Ph-BTP at different experimental conditions. Spiked with ^{241}Am(III) + ^{152}Eu(III) (1000 Bq each).

CONCLUSIONS

All studies performed until now point out towards SO_3-Ph-BTP aqueous phases show a better resistance against γ-irradiation when the irradiation takes place in contact with the organic phases (OK, TODGA in OK or TODGA-DMDOHEMA in OK), independently of the atmosphere and bubbled. Therefore, it would be the contact between phases and not the O_2 of the air-sparging who provides such protection. Besides, it seems that TODGA or TODGA-DMDOHEMA solvents could have a higher protector effect than kerosene over SO_3-Ph-BTP aqueous phase. Although estimation of SO_3-Ph-BTP concentrations has also been done, quantitative studies are still needed for all those systems where all factors involved cannot be isolated, as for example the hydrolysis of AHA.

Two reflections can be extracted as main conclusions from this work. On one hand, SO_3-Ph-BTP stability always should be considered taken into account the corresponding organic phase in contact. On the other hand, the effects of the presence of AHA in the aqueous phases must be depth-studied for a better understanding of the full system, since the An(II) seem to be better kept in the aqueous phase after irradiation, a reduction of D_{Eu} is observed reducing the An/Ln SF.

This project has received funding from the EURATOM research and training programme 2014-2018 under grant agreement No 755171. The content of this deliverable reflects only the author's view. The European Commission is not responsible for any use that may be made of the information it contains.

SO_3-PH-BTBP

KIT: A. Geist and C. Wagner

Stability of SO_3-Ph-BTBP vs. HNO_3 or alpha radiations

The SO_3-Ph-BTBP (Figure 12) AmSel (selective Am(III) extraction) system [23,24] was selected as a back-up for the EURO-EXAm process based on TPAEN.[25,26] Its stability in contact with nitric acid and under loading with Am(III) was studied.

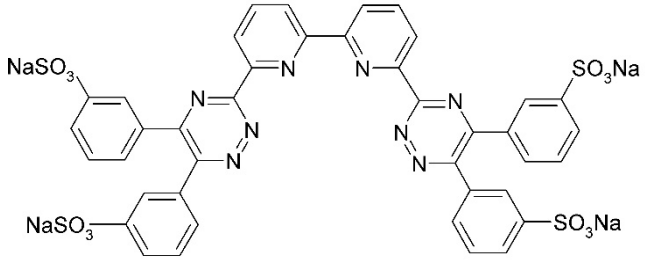

Figure 12: Molecular structure of SO_3-Ph-BTBP

STABILITY VS. HNO_3

Samples containing 20 mmol/L SO_3-Ph-BTBP in 0.5 or 2 mol/L HNO_3 and 0.2 mol/L TODGA + 5% 1-octanol in Exxsol D80 were spiked with ^{241}Am(III) and ^{154}Eu(III). The samples were kept for 63 days. Repeatedly the samples were placed on a shaker, centrifuged, and aliquots of both phases were taken for gamma analysis. The Am(III) and Eu(III) distribution ratios (Figure 13) remained practically constant, indicating sufficient chemical stability of this system. A similar behaviour (i.e. sufficient stability in contact with nitric acid) had already been observed for SO_3-Ph-BTP.[27]

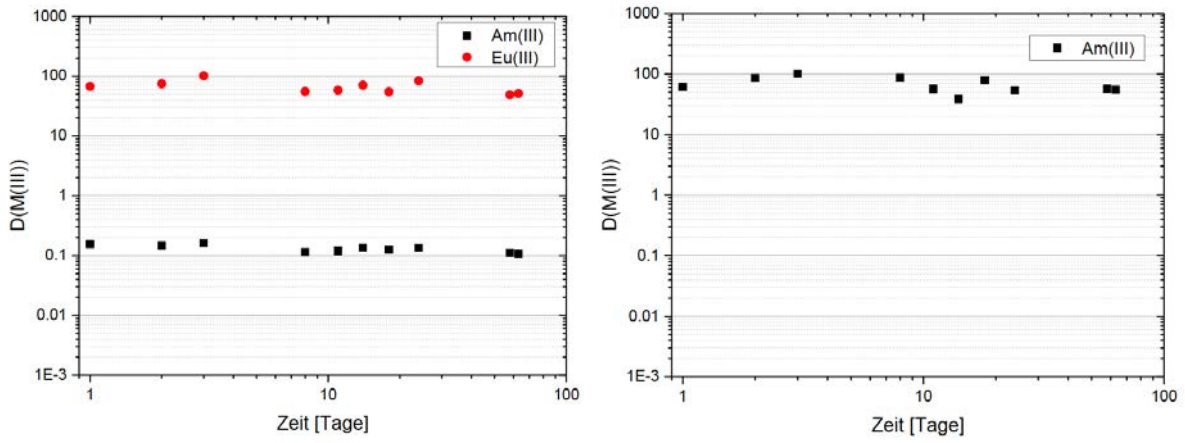

Figure 13. SO_3-Ph-BTBP stability vs. HNO_3. Organic phase, 0.2 mol/L TODGA + 5% octanol in Exxsol D80. Aqueous phase, 20 mmol/L SO_3-Ph-BTBP in 0.5 mol/L (top) or 2 mol/L (bottom) HNO_3. *T* = 293 K. *O/A* = 1.

This project has received funding from the EURATOM research and training programme 2014-2018 under grant agreement No 755171. The content of this deliverable reflects only the author's view. The European Commission is not responsible for any use that may be made of the information it contains.

STABILITY VS. ALPHA IRRADIATION

A solvent sample (0.2 mol/L TODGA + 5% octanol in Exxsol D80) loaded with 2.5 mmol/L ^{241,243}Am(III) was contacted with an aqueous solution containing 20 mmol/L SO_3-Ph-BTBP in 0.36 mol/L HNO_3, resulting in an equilibrium HNO_3 concentration of 0.5 mol/L and an aqueous phase Am(III) concentration of 2 mmol/L. No precipitation was observed for 21 days, resulting in an alpha dose of 10 kGy; Am(III) distribution ratio remained at $D_{Am(III)}$ = 0.2. However, after 60 days (28 kGy), Am(III) distribution ratio increased to $D_{Am(III)}$ = 0.44 and a pinkish precipitate was observed (Figure 14).

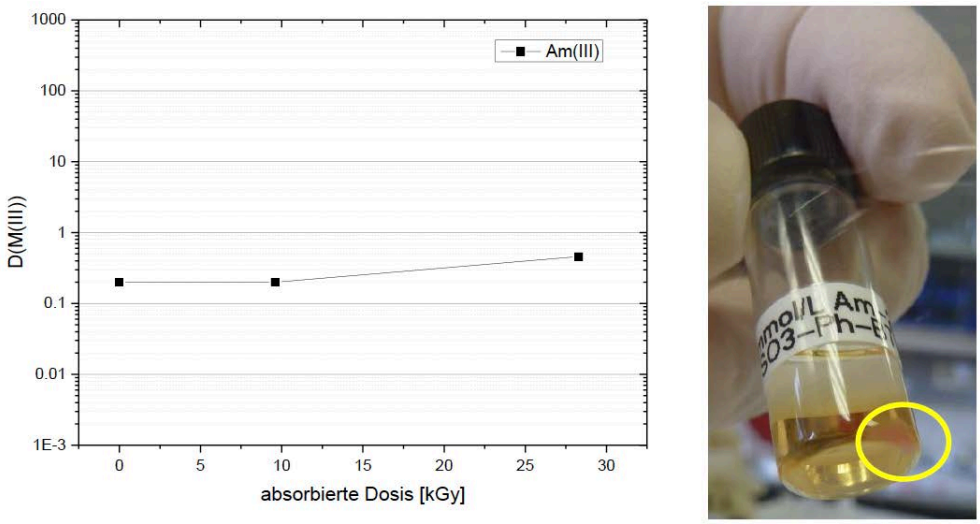

Figure 14. Left, Am(III) distribution ratio as a function of absorbed alpha dose. Organic phase, 0.2 mol/L TODGA + 5% octanol in Exxsol D80. Aqueous phase, 20 mmol/L SO_3-Ph-BTBP in 0.5 mol/L HNO_3. *T* = 293 K. *O/A* = 1. Right, Am(III) precipitate formed after 60 days, resulting in an alpha dose of 28 kGy.

CONCLUSIONS

Stripping agents such as SO_3-Ph-BTBP are intended as once-through reagents (i.e. they will not be recycled). Hence, their radiolytic stability is not a paramount concern, considering estimated alpha dose rates under process conditions which are below 1 kGy/h for typical UOx and MOx fuels.[28]

HYDROPHILIC DIGLYCOLAMIDES

(FZJ-Juelich: A. Wilden, D. Schneider, M. Gerdes, G. Modolo)

Short chain tetraethyldiglycolamides are, in general, water soluble molecules, and have been used as aqueous stripping and hold back agents, [29,30,31,32,33] as for example to strip lanthanides from the ALSEP solvent to regenerate that solvent for recycle, [30] or in EXAm process to enable a separation of the lanthanides and curium from americium. [31-33]

RADIOLYSIS & DEGRADATION PRODUCTS

DEGRADATION CHEMISTRY OF HYDROPHILIC DIGLYCOLAMIDES

This project has received funding from the EURATOM research and training programme 2014-2018 under grant agreement No 755171. The content of this deliverable reflects only the author's view. The European Commission is not responsible for any use that may be made of the information it contains.

The radiolysis of hydrophilic diglycolamides was studied in collaboration with Bruce Mincher (INL, USA) and Steve Mezyk (California State University Long Beach, USA). The radiolysis of TMDGA, TEDGA, Me-TEDGA, and Me_2-TEDGA was examined. The structures of the compounds used in this study are shown in Figure 15.

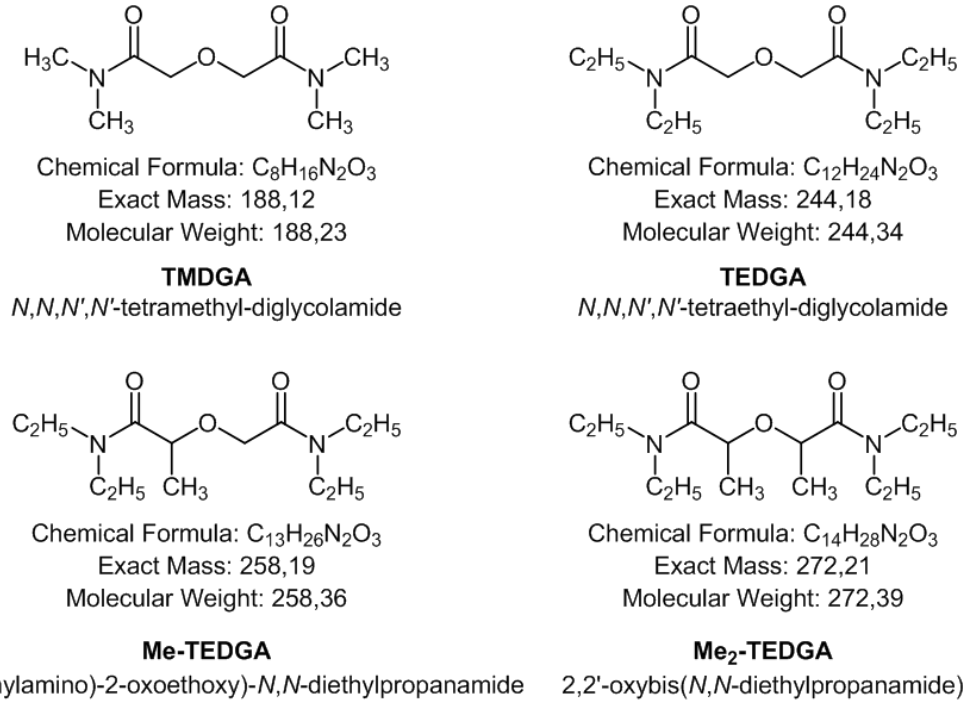

Figure 15. Chemical structures of the hydrophilic DGAs hydrolyzed and/or irradiated in this study.

Steady state γ-irradiations were performed at INL using a ^{60}Co-Nordion Gammacell 220, at a dose rate of 3.8 kGy h^{-1}, as initially measured using standard Fricke procedures, and then subsequently corrected for decay. The DGAs were irradiated as initially 0.05 M solutions in nanopure water to target absorbed doses of 0, 25, 50, 75, 100, 125 and 150 kGy, in sealed containers. Neutral water was chosen to allow for the study of radiolysis in the absence of the confounding hydrolysis effects expected in acidic solution. After irradiation the samples were delivered to FZJ for analysis. Irradiated samples were analyzed at FZJ by high performance liquid chromatography – electrospray ionization mass spectrometry/mass spectrometry (UHPLC-ESI-MS/MS). The chromatographic separations varied slightly with the DGA analyte. Product analysis was performed at FZJ using a hybrid linear ion trap FTICR (Fourier-Transform Ion Cyclotron Resonance) mass spectrometer LTQFT (Linear Tandem Quadrupole Fourier Transform) Ultra™ (Thermo Fisher Scientific, Bremen) coupled with an Agilent 1200 HPLC system. Mass spectra were recorded in full scan from 50 to 500 Da (TMDGA) or 100 to 1000 Da (TEDGA, Me-TEDGA, and Me_2-TEDGA) with a resolution of 100,000 at *m/z* 400.

The radiolytic decrease in all the hydrophilic DGAs examined was exponential with respect to absorbed dose. This is shown in Figure 16 using initially 0.05 mol/L TEDGA as an example, and is consistent with the kinetics reported in our previous work with lipophilic DGAs. [34,35,36] The dose constant *d* from Figure 16 is 11.1 x 10^{-3} kGy^{-1}, which corresponds to a G_o-value of 0.56 µmol J^{-1}. A replicate set of irradiations resulted in *d* = 9.5 x 10^{-3}, and G_o = 0.48 µmol J^{-1}, for mean values of (10.3 ± 1.13) x 10^{-3} kGy^{-1}, and 0.52 ± 0.06 µmol J^{-1}. This rate of radiolytic degradation is about twice that reported for lipophilic DGAs such as TODGA and TEHDGA [34], D^3DODGA [35], and the methylated TODGAs [36]. These values, and those for the other hydrophilic DGAs are shown in Table 5.

This project has received funding from the EURATOM research and training programme 2014-2018 under grant agreement No 755171. The content of this deliverable reflects only the author's view. The European Commission is not responsible for any use that may be made of the information it contains.

It can be seen in Table 5 that the degradation rates decreased with the increasing molecular weight, following the trend TMDGA > TEDGA > Me-TEDGA > Me_2-TEDGA.

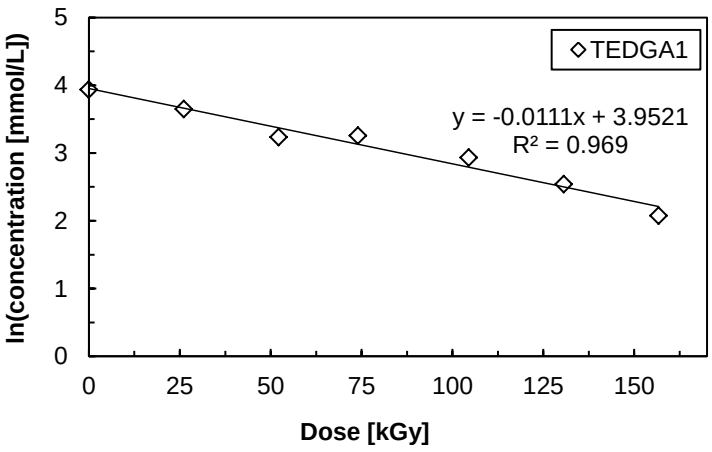

Figure 16. The plot of TEDGA concentration in water for initially 0.05 M TEDGA, versus absorbed radiation dose.

Table 5. Dose constants for the degradation of hydrophilic diglycolamides.

Diglycolamide	Dose constant *d* (kGy^{-1})	G_0 ($\mu mol\ J^{-1}$)
TMDGA	14.9×10^{-3}	0.75
TEDGA trial 1	11.1×10^{-3}	0.56
TEDGA trial 2	9.5×10^{-3}	0.48
Me-TEDGA	7.8×10^{-3}	0.39
Me_2-TEDGA	7.3×10^{-3}	0.37

Dose constants have now also been reported for many lipophilic DGAs over a range of carbon chain lengths and the degradation rates were similar for samples irradiated under a variety of conditions including in pure dodecane solution, when in contact with aqueous phases of varying acidity or in the presence or absence of air sparging.[34,35,36] Their values are similar and slower than the values reported for the hydrophilic DGAs in Table 5.

Irradiated samples of the different hydrophilic diglycolamides were analyzed by HPLC-MS using a high resolution mass spectrometer. The high resolution enabled an identification of the radiolysis products by their molecular weights (more precisely the m/z ratios) and the corresponding chemical formulae. Furthermore, the intensity of the degradation products was followed as a function of the absorbed dose by measuring the area of the corresponding peaks in the chromatograms when only the derived *m/z* ratio was monitored. Although this method is not precisely quantitative, as ionization potentials are different for different fragments and also depending on the total ion count, a rough estimate of the quantity in the samples can be given. The *m/z* ratios of the protonated degradation product ions were used, although also sodiated product ions, adducts with NH_4^+ ions as well as higher complexes (e.g. 1:2 Na:ligand complexes) where observed.

Analogous products were identified for the radiolysis of all hydrophilic DGAs examined, and they are partly consistent with the products found for the irradiation of lipophilic DGAs. [34,35,36] Figure 17 shows a schematic representation of possible degradation reactions and the corresponding product spectrum.

This project has received funding from the EURATOM research and training programme 2014-2018 under grant agreement No 755171. The content of this deliverable reflects only the author's view. The European Commission is not responsible for any use that may be made of the information it contains.

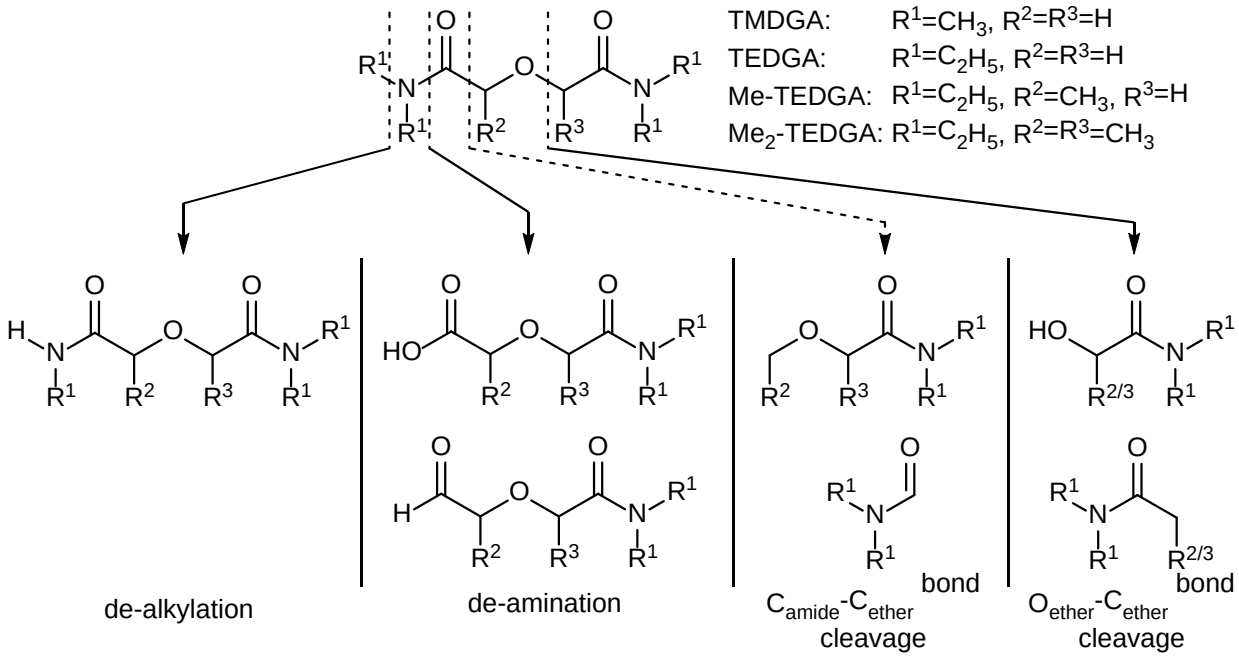

Figure 17. Schematic representation of possible degradation reactions and corresponding product spectrum.

De-alkylation products were identified for all hydrophilic DGAs, both for single and double de-alkylation reactions. Single de-alkylations were the most prominent reactions with the products showing a clear concentration increase with increasing dose. Either no or very little of these products were found in the unirradiated samples. Products of a double de-alkylation reaction have also been identified and they show a similar increase in concentration with increasing dose, although their concentration is much lower than that of the single de-alkylation reaction. The double de-alkylation degradation fragment can be formed by two de-alkylations of a single amidic nitrogen atom or by two single de-alkylations of two different amidic nitrogen atoms. It's not possible to distinguish between these two paths by the analytical method used here, but the appearance of more than one peak in some chromatograms could be interpreted as both reactions having taken place. Products of a triple or quadruple de-alkylation were not found. Similar de-alkylation reactions have been reported for various lipophilic DGAs[34,35,36], CMPO [37] and TBP [38].

Products of the de-amination reaction (carboxylic acids shown in Figure 17) have been found in all irradiated samples. These compounds were also identified in the unirradiated samples and are therefore probably partly left-over from the synthesis. However, the concentration in the irradiated samples was higher and generally increased with absorbed dose. An acidic product, resulting from the amide hydrolysis, such as this could be an important complexing agent that might interfere with separations. The potential reduction product (aldehyde) shown in Figure 17 was not detected, since these conditions usually give oxidation and not reduction products. The other product of the de-amination reaction is a secondary amine. These amines could not be detected, as their masses were too low and out of the mass range measured in this study.

Possible products of a C_{amide}-C_{ether} bond cleavage could not be identified. Although such products were reported for lipophilic DGAs [34,35,36] they occurred at low abundance. Thus it is concluded that C-C bond ruptures are relatively rare decomposition modes for the DGAs in both diluents.

This project has received funding from the EURATOM research and training programme 2014-2018 under grant agreement No 755171. The content of this deliverable reflects only the author's view. The European Commission is not responsible for any use that may be made of the information it contains.

The alcohols formed through O_{ether}-C_{ether} bond cleavage were identified in all irradiated samples except the TMDGA samples, and their intensities increased with increasing absorbed dose. It is not clear why the alcohols were not detectable in the irradiated TMDGA samples. However, this suggests that the initiation of the events leading to ether bond rupture occur in the side chains, specifically on a $\geq$ secondary carbon atom. Such an initiation event could be H-atom abstraction from the carbon atom, to be discussed in more detail later. Abstraction of an H-atom from the methyl carbon atoms of TMDGA is expected to be more difficult than for abstraction of H-atoms from the methylene carbons in the longer alkane chains.

The secondary products of O_{ether}-C_{ether} bond cleavage balancing the molecules are low molecular weight acetamides, but have not been detected. This may indicate that they undergo hydrolysis or rapid radiolysis upon production and is different to the lipophilic DGAs irradiated in organic diluent, where these products have been identified. [34,35,36]

Products corresponding to the hydroxylation of the DGAs were also detected. The two types detected include hydroxylation of the DGA itself, but also hydroxylated dealkylation products. They were found in all irradiated samples and were absent in the unirradiated samples. Except for TMDGA, the intensity of these products increased with increasing dose. In the TMDGA case, a high quantity was observed in the first samples and the intensity decreased slightly upon continued irradiation. This is also consistent with H-atom abstraction being difficult for the methyl carbons of TMDGA. The initial H-atom abstractions followed by •OH radical addition occur only for the two methylene carbon positions on TMDGA. Continued radiolysis does not provide additional opportunity for hydroxylation of this compound.

Interesting products with *m/z* ratios corresponding to the combination of the products of the single de-alkylation and the alcohol radical formed by O_{ether}-C_{ether} bond cleavage were detected. They are attributed to an addition reaction between the radicals initially produced by these bond ruptures, with the corresponding reaction scheme shown in Figure 18. The intensities of these recombination products increase with increasing dose and they are not detected in the unirradiated samples. They were found in all irradiated samples except those of TMDGA. This is consistent with the absence of products of O_{ether}-C_{ether} bond cleavage in the irradiated TMDGA samples.

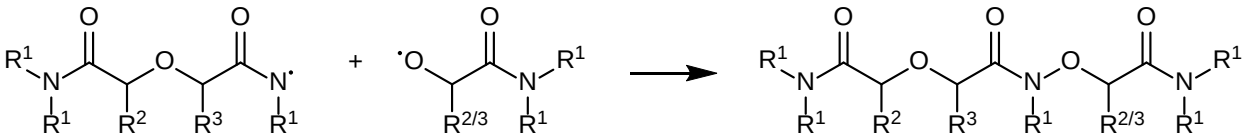

TMDGA: $R^1=CH_3$, $R^2=R^3=H$
TEDGA: $R^1=C_2H_5$, $R^2=R^3=H$
Me-TEDGA: $R^1=C_2H_5$, $R^2=CH_3$, $R^3=H$
Me_2-TEDGA: $R^1=C_2H_5$, $R^2=R^3=CH_3$

Figure 18. Reaction scheme of the combination reaction of the single de-alkylation product radical with the alcohol radical formed by O_{ether}-C_{ether} bond cleavage.

Additionally, *m/z* ratios were observed that could correspond to acetylated molecules of the de-alkylation products. However, it is believed that these products were formed during the analysis, as their retention times were nearly identical to the parent molecules.

This project has received funding from the EURATOM research and training programme 2014-2018 under grant agreement No 755171. The content of this deliverable reflects only the author's view. The European Commission is not responsible for any use that may be made of the information it contains.

PTD

PTD STABILITY

(POLIMI: E. Macerata, E. Mossini, M. Mariani, A. Ossola, M. Giola)

INTRODUCTION

The water-soluble ligands (PyTri-polyols) with the 2,6-bis[1H-1,2,3-triazol-4-yl]-pyridine chelating unit have been designed as minor actinides stripping agents with promising results [39, 40]. Several studies were performed on the stripping solvent formulation consisting of 0.08 mol L^{-1} PyTri-Diol (PTD) dissolved in 0.44 mol L^{-1} HNO_3, in order to assess its stability under the harsh conditions of the partitioning i-SANEX and GANEX processes. In particular, stability toward aging, hydrolysis and radiolysis has been herein extensively investigating.

PTD STABILITY TOWARD AGING AND HYDROLYSIS

In order to investigate the ligand stability in the acidic medium, PTD stripping solutions were left to age in the dark at ambient temperature for several months, up to approximately one year. Solvent extraction tests and HPLC-MS analyses were performed to assess the performance and ascertain if ligand degradation occurred. All experiments were carried out following standard protocols. In liquid-liquid extraction experiments, the 3 mol L^{-1} HNO_3 feed solution was spiked with $^{241}Am(III)$ and $^{152}Eu(III)$, chosen as representatives of Actinides (An) and Lanthanides (Ln) respectively. As it could be inferred from Figure 19, the distribution ratio of Am(III) is consistently below unity and that of Eu(III) above unity, so that it could be concluded that the system maintains its performance if aged up to 321 days. Furthermore, the results of HPLC-ESI-MS analyses confirms this result (Figure 20). In fact, no ligand by-products were identified and the ligand concentration was maintained as in the fresh ligand solution.

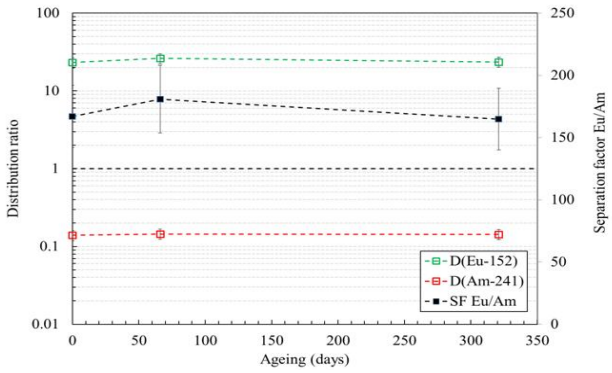

Figure 19: Distribution ratios of $^{241}Am(III)$ and $^{152}Eu(III)$ and Eu/Am separation factor as a function of aqueous stripping phase ageing. Organic phase: 0.2 mol L^{-1} TODGA in kerosene with 5 vol% 1-octanol loaded from 3 mol L^{-1} HNO_3 spiked with $^{241}Am(III)$ and $^{15}2Eu(III)$ and scrubbed with 0.5 mol L^{-1} HNO_3. Aqueous stripping phase: 0.08 mol L^{-1} PTD in 0.44 mol L^{-1} HNO_3 pre-equilibrated with 0.2 mol L^{-1} TODGA in kerosene with 5 vol% 1-octanol. The stripping phases were aged in the dark at ambient temperature (22 ± 2°C) for 66 and 321 days.

This project has received funding from the EURATOM research and training programme 2014-2018 under grant agreement No 755171. The content of this deliverable reflects only the author's view. The European Commission is not responsible for any use that may be made of the information it contains.

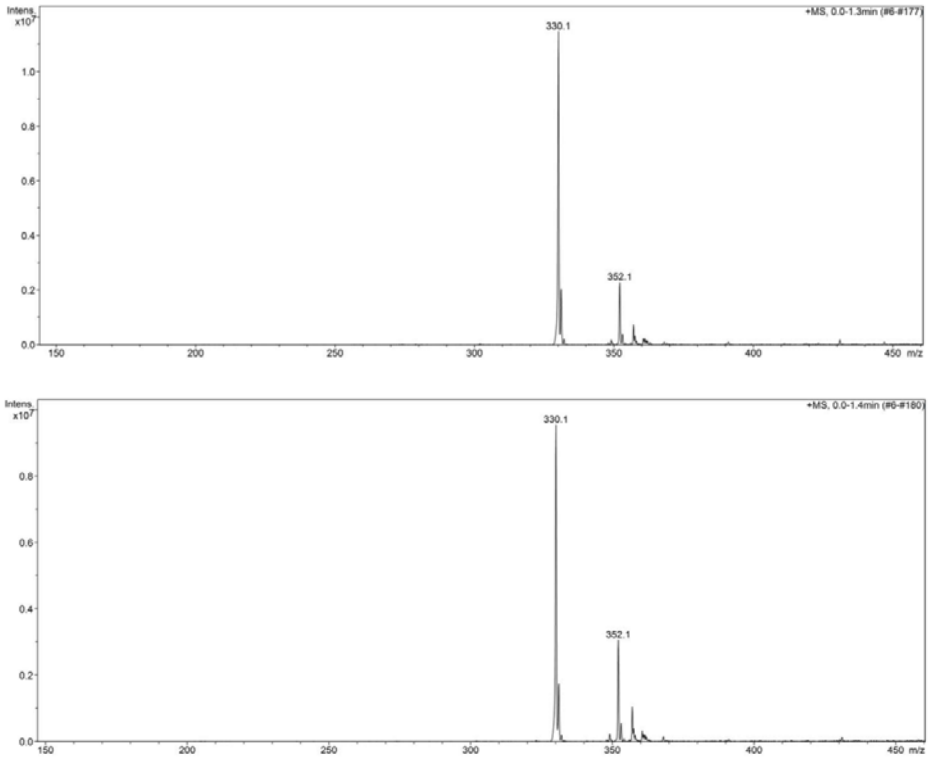

Figure 20: ESI-MS spectra obtained by direct infusion of (*top*) fresh 0.08 mol L^{-1} PTD in 0.44 mol L^{-1} HNO_3, after proper dilution in methanol; and (*bottom*) of aged 0.08 mol L^{-1} PTD in 0.44 mol L^{-1} HNO_3 pre-equilibrated with 0.2 mol L^{-1} TODGA in kerosene with 5 vol% 1-octanol, after proper dilution in methanol. The PTD solution was aged in the dark at ambient temperature (22 ± 2°C) for 321 days.

Furthermore, hydrolytical stability of PTD aged in the dark at ambient temperature in about 5 M HNO_3 has been checked by ESI-MS analysis. The spectra of fresh and 25 days aged PTD are reported in Figures 21 and 22. The primary peaks were the $PTDH^+$ adduct at 330 m/z and the $PTDNa^+$ adduct at 352 m/z. As it could be evidenced, no hydrolytic by-products are formed due to ageing in 5 M HNO_3. The 274.1 and 302.1 m/z should not be associated to hydrolytic by-products, but to undesired ligand fragments produced during the ionization process, in agreement with MS^2 spectra of ligand proton and sodium adducts.

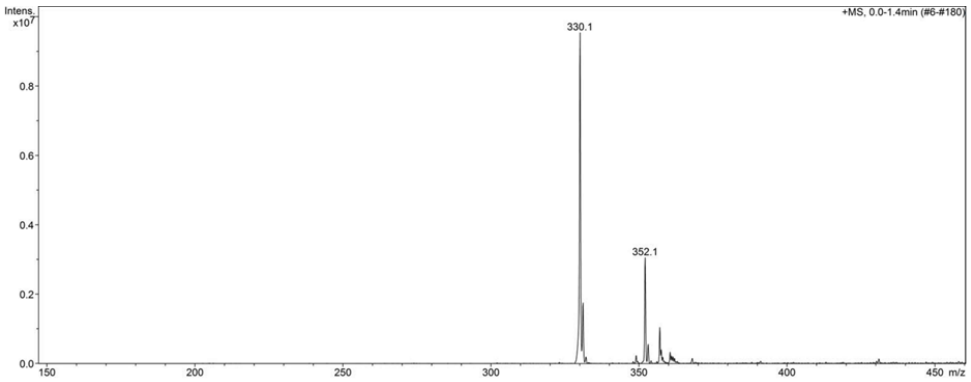

Figure 21: Positive ESI-MS spectrum of fresh PTD diluted in methanol. 330.1 m/z and 352.1 m/z represents the PTD proton and sodium adducts.

This project has received funding from the EURATOM research and training programme 2014-2018 under grant agreement No 755171. The content of this deliverable reflects only the author's view. The European Commission is not responsible for any use that may be made of the information it contains.

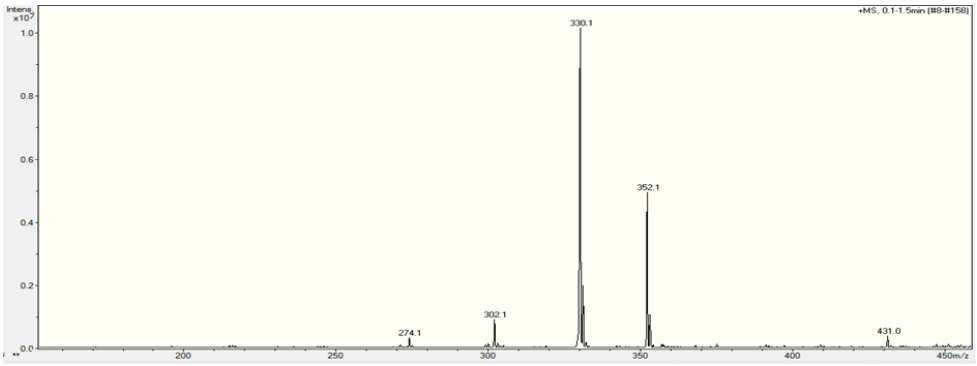

Figure 22: Positive ESI-MS spectrum of PTD aged in about 5 M HNO_3 for 25 days and diluted in methanol. 330.1 m/z and 352.1 m/z represents the PTD proton and sodium adducts.

PTD STABILITY TOWARD RADIOLYSIS

In order to investigate the ligand stability towards radiolysis, PTD stripping solutions were irradiated by two ^{60}Co sources characterized by different dose rates: 2.5 and 0.13 kGy h^{-1}. The samples were stored in 4 mL glass vials closed with a plastic lid and sealed with Parafilm® in order to avoid sample leakage during irradiation. The irradiations were performed in the dark at ambient temperature. Irradiated samples were kept in the dark at ambient temperature till the end of the longest irradiation, while at the end of the irradiation campaign, all samples were stored in the dark at 4 ± 1°C until further analysis. Therefore, all the samples of each irradiation campaign were subjected to the same thermal history.

Impact on extracting performances

First, preliminary irradiations of the PTD stripping solutions, not pre-equilibrated with the TODGA organic phase, were performed up to absorbed dose of 500 kGy with the 2.5 kGy/h ^{60}Co source and up to 100 kGy with the 0.13 kGy/h ^{60}Co source.

Solvent extraction tests were performed to assess the performance of irradiated PTD solutions in presence of different feeds: one consisting of 3 mol L^{-1} HNO_3 (feed I) and another containing, coherently with the PUREX raffinate composition, 2.49 g/L of yttrium and Ln (from lanthanum to gadolinium) in 3 mol L^{-1} HNO_3 (feed II). Trace amounts of selected radionuclides (10 kBq mL^{-1} each) were added, $^{239}Pu(IV)$, $^{241}Am(III)$ and $^{244}Cm(III)$ as representative of An and $^{152}Eu(III)$ for Ln. The results obtained with feed I spiked with $^{241}Am(III)$ and $^{152}Eu(III)$ are reported in Figure 23. If PTD is irradiated at 500 kGy, the distribution ratios of $^{241}Am(III)$, and even more so $^{152}Eu(III)$, considerably decrease, leading to a severe reduction of the Eu/Am separation factor from about 200 to 66. The results obtained with feed II spiked with $^{241}Am(III)$ and $^{152}Eu(III)$ are reported in Figure 24, while those with $^{239}Pu(IV)$, $^{241}Am(III)$, $^{244}Cm(III)$ and $^{152}Eu(III)$ are reported in Figure 25. As it could be deduced from the graphs, the distribution ratios of radiotracers and stable Ln are almost constant within the absorbed dose range considered. The TODGA-PTD system is able to perform the An/Ln separation if the stripping solution is irradiated up to 200 kGy.

This project has received funding from the EURATOM research and training programme 2014-2018 under grant agreement No 755171. The content of this deliverable reflects only the author's view. The European Commission is not responsible for any use that may be made of the information it contains.

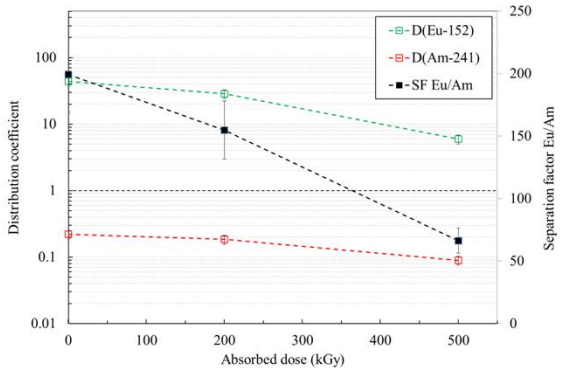

Figure 23: Distribution ratios of ^{241}Am(III) and ^{152}Eu(III) and Eu/Am separation factor as a function of absorbed dose. Organic phase: 0.2 mol L^{-1} TODGA in kerosene with 5 vol% 1-octanol loaded from feed I spiked with ^{241}Am(III) and ^{152}Eu(III) and scrubbed with 0.5 mol L^{-1} HNO_3. Aqueous stripping phases: 0.08 mol L^{-1} PTD in 0.44 mol L^{-1} HNO_3. The irradiation of aqueous phase was performed with 2.5 kGy h^{-1} dose rate ^{60}Co source.

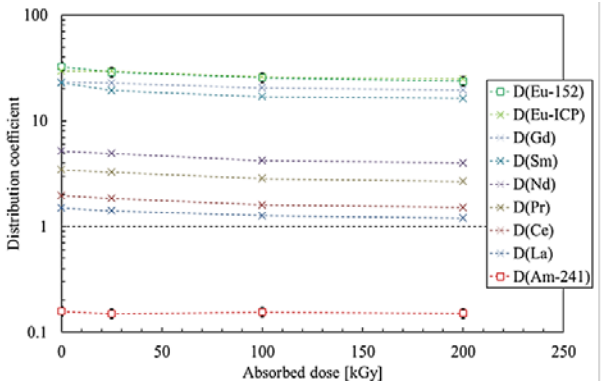

Figure 24: Distribution ratios of ^{241}Am(III) and Ln(III) as a function of absorbed dose. Organic phase: 0.2 mol L^{-1} TODGA in kerosene with 5 vol% 1-octanol loaded from feed II spiked with ^{241}Am(III) and ^{152}Eu(III) and scrubbed with 0.5 mol L^{-1} HNO_3. Aqueous stripping phases: 0.08 mol L^{-1} PTD in 0.44 mol L^{-1} HNO_3. The irradiation was performed with 2.5 kGy h^{-1} dose rate ^{60}Co source.

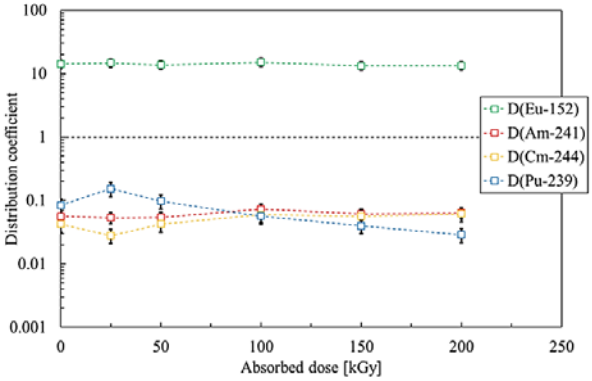

Figure 25: Distribution ratios of ^{241}Am(III), ^{244}Cm(III), ^{239}Pu(IV), ^{152}Eu(III) as a function of absorbed dose. Organic phase: 0.2 mol L^{-1} TODGA in kerosene with 5 vol% 1-octanol loaded from feed II spiked with ^{241}Am(III), ^{244}Cm(III), ^{239}Pu(IV), ^{152}Eu(III) at 3 mol L^{-1} HNO_3 and scrubbed with 0.5 mol L^{-1} HNO_3. Aqueous stripping phases: 0.08 mol L^{-1} PTD in 0.44 mol L^{-1} HNO_3. The irradiation was performed with 2.5 kGy h^{-1} dose rate ^{60}Co source.

This project has received funding from the EURATOM research and training programme 2014-2018 under grant agreement No 755171. The content of this deliverable reflects only the author's view. The European Commission is not responsible for any use that may be made of the information it contains.

Afterwards, PTD solutions pre-equilibrated with two different organic phases (kerosene with 5 vol% 1-octanol and 0.2 mol L^{-1} TODGA in kerosene with 5 vol% 1-octanol) were aged (for 66 days) or irradiated (at 200 kGy) with the 2.5 kGy h^{-1} ^{60}Co source. The results of the liquid-liquid extraction experiments with the differently pre-equilibrated PTD solutions are reported in Figures 26 and 27. It could be inferred that ageing does not produce any performance degradation, while a slight reduction of the $^{152}Eu(III)$ distribution ratio and, consequently, the Eu/Am separation factor occurred after PTD solutions irradiation at 200 kGy. This is more than enough for an aqueous phase, which will be not recycled.

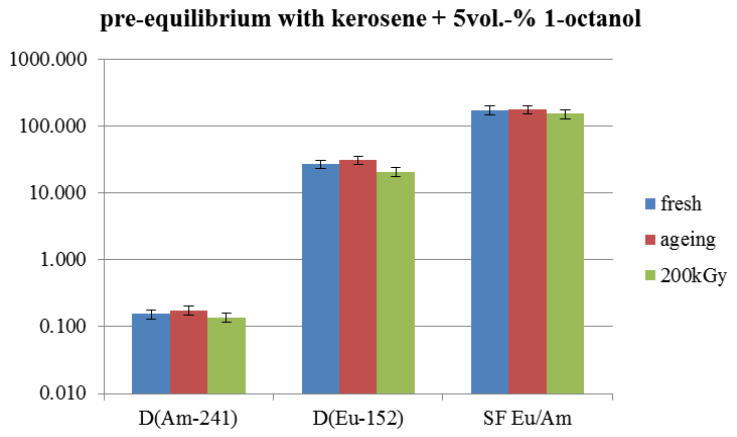

Figure 26: Distribution ratios of $^{241}Am(III)$ and $^{152}Eu(III)$ and Eu/Am separation factor as a function of absorbed dose. Organic phase: 0.2 mol L^{-1} TODGA in kerosene with 5 vol% 1-octanol loaded from feed I spiked with $^{241}Am(III)$ and $^{152}Eu(III)$ and scrubbed with 0.5 mol L^{-1} HNO_3. Aqueous stripping phases: 0.08 mol L^{-1} PTD in 0.44 mol L^{-1} HNO_3 pre-equilibrated with kerosene + 5vol% 1-octanol before irradiation with 2.5 kGy h^{-1} dose rate ^{60}Co source.

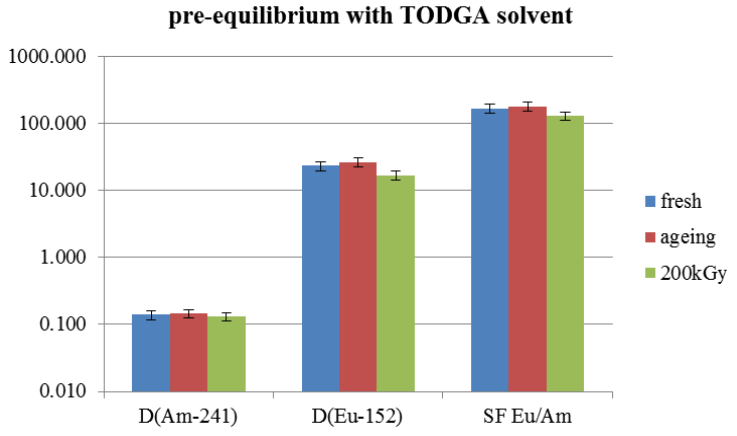

Figure 27: Distribution ratios of $^{241}Am(III)$ and $^{152}Eu(III)$ and Eu/Am separation factor as a function of absorbed dose. Organic phase: 0.2 mol L^{-1} TODGA in kerosene with 5 vol% 1-octanol loaded from feed I spiked with $^{241}Am(III)$ and $^{152}Eu(III)$ and scrubbed with 0.5 mol L^{-1} HNO_3. Aqueous stripping phases: 0.08 mol L^{-1} PTD in 0.44 mol L^{-1} HNO_3 pre-equilibrated with 0.2 mol L^{-1} TODGA in kerosene + 5vol% 1-octanol before irradiation with 2.5 kGy h^{-1} dose rate ^{60}Co source.

Within a collaboration with the Laboratories of CEA in Marcoule, the loading capability of PTD-based stripping solutions has been assessed and verified also with aged and irradiated PTD solutions. In view of the application

This project has received funding from the EURATOM research and training programme 2014-2018 under grant agreement No 755171. The content of this deliverable reflects only the author's view. The European Commission is not responsible for any use that may be made of the information it contains.

in the *i*-SANEX process, americium loading capability of PTD was investigated by means of liquid-liquid extraction experiments with a 3 mol L^{-1} nitric acid aqueous feed containing macro-concentrations of Am and lanthanides (0.001 mol L^{-1} ^{241}Am(III), 0.02 mol L^{-1} of trivalent Y and Ln (La-Gd), ^{152}Eu(III) as radiotracer). The i-SANEX reference organic solvent (0.2 M TODGA in kerosene + 5 vol% 1-octanol) was loaded from this aqueous feed, afterwards scrubbed with 0.5 M nitric acid and utilized to perform the stripping tests. Figure 28 reports the results obtained from the Am loading experiments. Ligand performances were evaluated by executing stripping tests with 0.08 mol L^{-1} PTD in 0.44 mol L^{-1} HNO_3 fresh, aged (for around 1 month) and irradiated (up to 200 kGy) solutions, at the controlled temperature of 25°C. Stripping tests with only 0.44 mol L^{-1} HNO_3 were performed as references. Remarkably, as appreciable from Figure 28, PTD is still able to selectively re-extract americium even in macro-concentration. In fact, as in the case of spiked experiments, by comparing the results of tests i and ii (Figure 28), the addition of just 0.08 mol L^{-1} PTD is capable of substantially reducing Am D value below 1, while Eu D value remains far above 1. Furthermore, ^{241}Am and ^{152}Eu distribution ratios resulted to be almost unaltered towards ageing and irradiation (radiolysis) with separation factors between ^{152}Eu and ^{241}Am around 200 in all the conditions tested. No variation from the results obtained with spiked tests were highlighted.

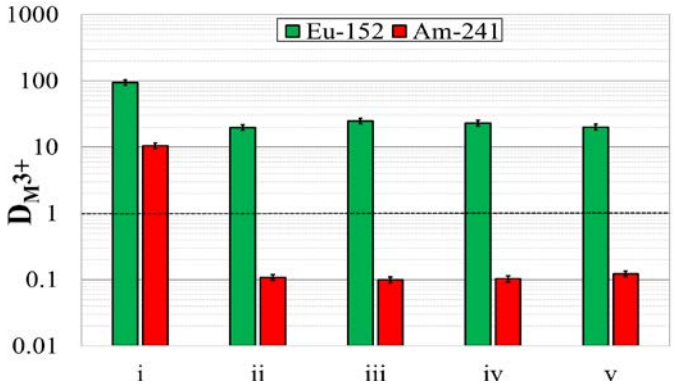

Figure 28: Distribution ratios of trivalent ^{241}Am and ^{152}Eu obtained by contacting loaded TODGA solutions with the following stripping solutions: i) fresh 0.44 mol L^{-1} HNO_3, ii) fresh PTD, iii) aged PTD, iv) PTD irradiated at 100 kGy and v) PTD irradiated at 200 kGy.

Identification of the degradation products

In order to investigate the degradation of the irradiated PTD solutions, preliminary ESI-MS analyses of irradiated PTD solutions were performed. The spectra obtained with fresh and irradiated (200 kGy with the 2.5 kGy h^{-1} ^{60}Co source) PTD solutions are reported in Figure 29. As it could be observed, few new species appear in the spectrum of the irradiated solution at m/z 343.7, 360, 382.1, 391.6 and 406.1. With the purpose of deepen the comprehension about PTD degradation, HPLC-ESI-MS analyses were performed. Thanks to the coupling between the HPLC and the ESI-MS equipment, several degradation by-products were observed. The ion chromatograms of both the ligand and the by-products species were extracted. The percentage PTD concentration in the solutions irradiated by 2.5 and 0.13 kGy h^{-1} ^{60}Co sources was estimated with respect to the total ion current and is reported as a function of the absorbed dose in Figure 30 and Figure 31, respectively.

This project has received funding from the EURATOM research and training programme 2014-2018 under grant agreement No 755171. The content of this deliverable reflects only the author's view. The European Commission is not responsible for any use that may be made of the information it contains.

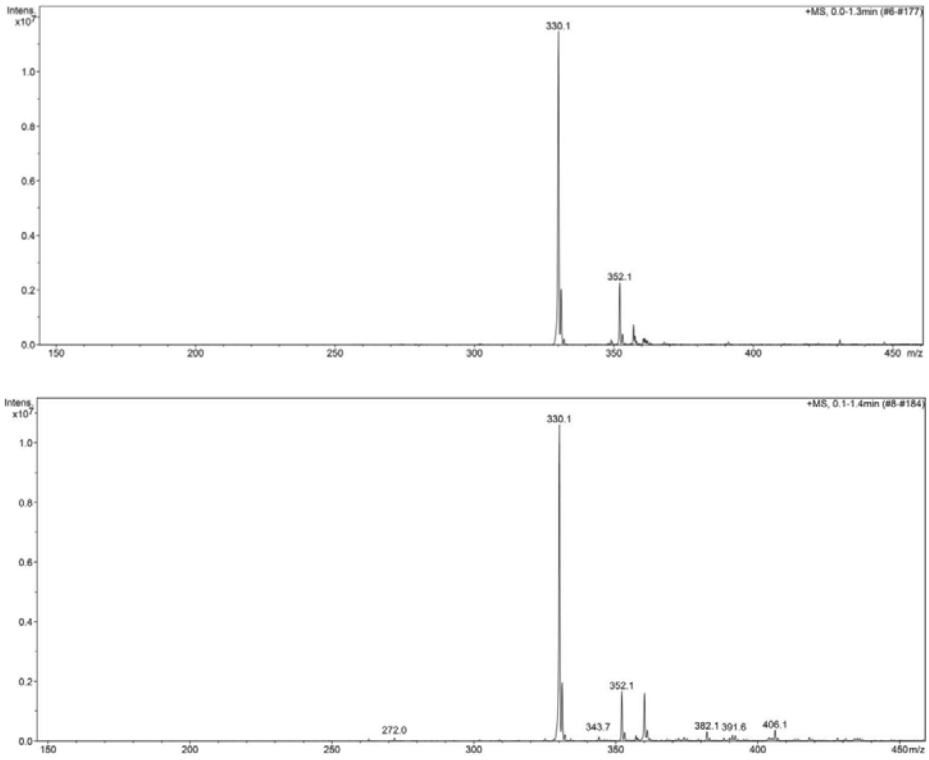

Figure 29: ESI-MS spectra obtained by direct infusion of (*top*) fresh 0.08 mol L^{-1} PTD in 0.44 mol L^{-1} HNO_3 and (*bottom*) irradiated 0.08 mol L^{-1} PTD in 0.44 mol L^{-1} HNO_3, after proper dilution in methanol. The irradiation was performed with 2.5 kGy h^{-1} dose rate ^{60}Co source.

Compared with the unirradiated reference sample, the ligand concentration decrease was estimated to be about 12% and 25% in samples irradiated at high dose rate at 200 and 500 kGy, respectively. While at low dose rate a decrease of about 12% was observed already at 100 kGy. The ligand concentration decrease can be interpolated with a linear fit in all the dose range for the irradiations at low dose rate and up to 200kGy at high dose rate. The consumption yields (G-values) were estimated and turned out to be - 0.048 +/- 0.004 µmol J^{-1} and -0.103 ± 0.003 µmol J^{-1} at higher and lower dose rate, respectively.

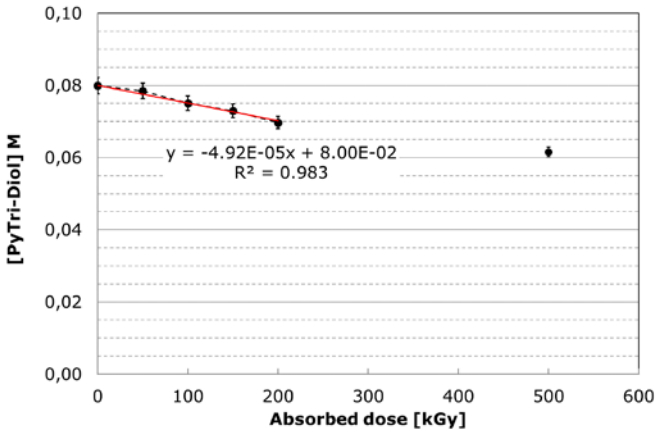

Figure 30: Percentage of initial PTD as a function of the absorbed dose by HPLC-ESI-MS analyses. Solutions of 0.08 mol L^{-1} PTD in 0.44 mol L^{-1} HNO_3 were irradiated with 2.5 kGy h^{-1} dose rate ^{60}Co source.

This project has received funding from the EURATOM research and training programme 2014-2018 under grant agreement No 755171. The content of this deliverable reflects only the author's view. The European Commission is not responsible for any use that may be made of the information it contains.

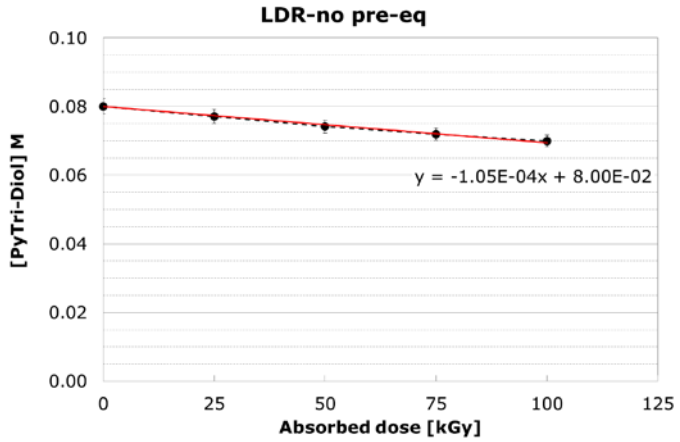

Figure 31: Percentage of initial PTD as a function of the absorbed dose by HPLC-ESI-MS analyses. Solutions of 0.08 mol L^{-1} PTD in 0.44 mol L^{-1} HNO_3 were irradiated with 0.13 kGy h^{-1} dose rate ^{60}Co source.

Similarly, to the assessment of the PTD concentration following irradiation, a semi-quantitative evaluation of the observed by-products was performed. The percentage of each by-product in both aged and irradiated PTD solutions was estimated considering the respective ion current and dividing it by the total ion current. It was demonstrated that the degradation by-products are not formed in PTD solutions aged up to 321 days. On the other hand, the results obtained with PTD solutions pre-equilibrated with 0.2 mol L^{-1} TODGA in kerosene with 5 vol% 1-octanol irradiated up to 500 kGy with the 2.5 kGy h^{-1} ^{60}Co source are reported in Figure 32. As it could be inferred from the graph, the by-product percentages increase with the absorbed dose.

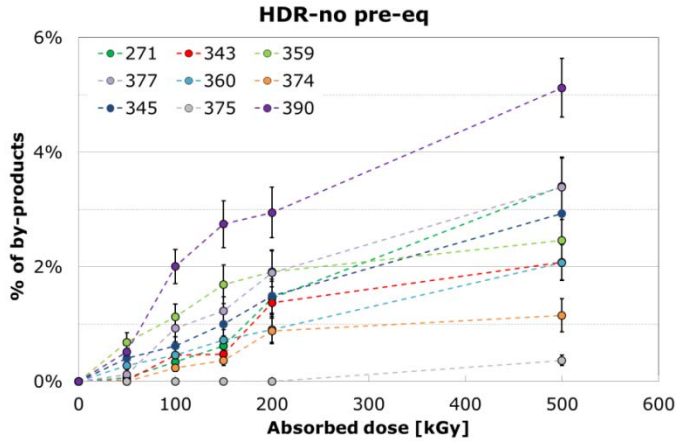

Figure 32: Percentage of PTD by-products as a function of the absorbed dose by HPLC-ESI-MS analysis. Solutions of 0.08 mol L^{-1} PTD in 0.44 mol L^{-1} HNO_3 were irradiated with 2.5 kGy h^{-1} dose rate ^{60}Co source.

On the basis of radiation chemistry literature and the mass tandem spectrometry experiments, plausible molecular structures have been proposed as reported in Figure 33. The lateral branches have been supposed to be the weakest position of the ligand structure, while the aromatic moieties the most radiation resistant one. The ligand degradation has been considered mainly caused by indirect reaction with radiolytic species of the diluent (water and nitric acid). Consequently, to the most probable reaction of hydrogen atom abstraction from the C-H bond in alpha position with respect to the triazolyl ring or to the alcoholic group, the proposed degradation paths entail the addition of radical species coming from diluent radiolysis. On the other hand, the branch loss could follow hydrogen atom abstraction from the alpha position adjacent to the triazolyl ring. The

This project has received funding from the EURATOM research and training programme 2014-2018 under grant agreement No 755171. The content of this deliverable reflects only the author's view. The European Commission is not responsible for any use that may be made of the information it contains.

proposed PTD by-products structures are compatible with the liquid-liquid extraction results, since it is evident that both complexing ability and solubility of these by-products should be similar to those of PTD.

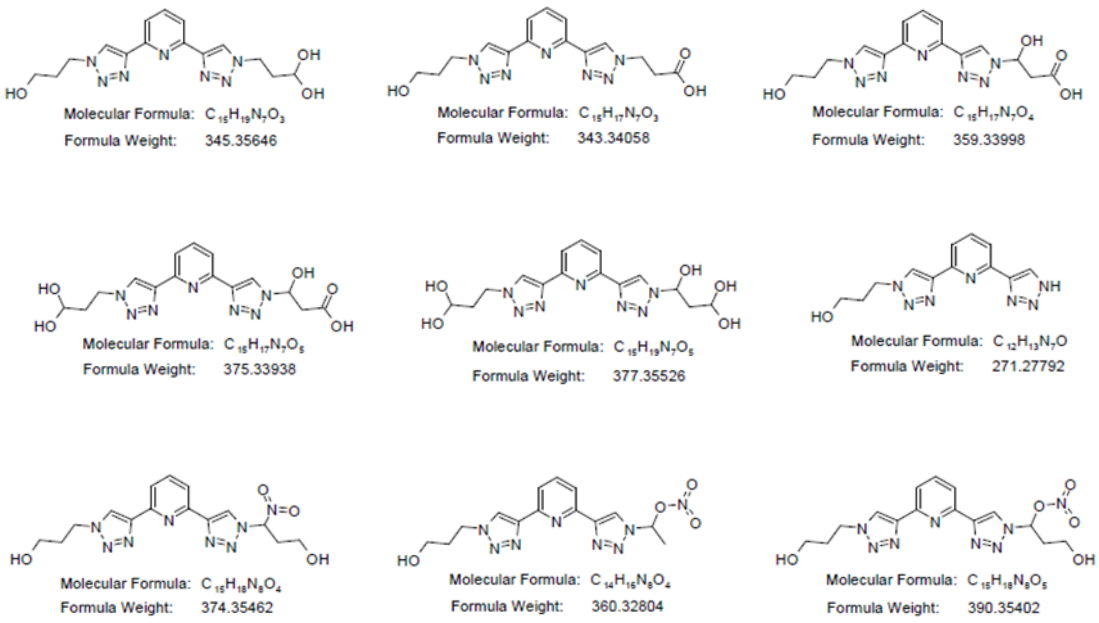

Figure 33: Hypothesised structures of identified PTD by-products.

COMPARISON OF GAMMA AND ALPHA IRRADIATION

(CEA & POLIMI: A. Kimberlin, A. Ossola, G. Saint-Louis, D. Guillaumont, P. Guilbaud & L. Berthon)

INTRODUCTION

A study was done in order to better understand the degradation mechanisms and degradation products pathways of the PyTri-Diol (PTD) complexing agent using ESI-MS analysis and DFT calculations. Experiments using gamma and alpha irradiations were performed in order to compare their impact on the degradation product formation, and DFT calculation were done in order to calculate the Fukui functions that give insight on the possible electrophilic, nucleophilic, or radical attack on a molecule. Gamma irradiations and aged samples were prepared by Annalisa Ossola (POLIMI). Alpha irradiation and DFT calculations were done in the ATALANTE facility (CEA).

ANALYSIS OF INTACT PTD AND AGED PTD SOLUTIONS

The stability of PTD was first assessed toward hydrolysis (i.e. in nitric acid solution, without any radiation effect). These tests are substantially similar to those duplicated later on and more extensively at CEA and reported on page 21. ESI-MS analysis was performed on fresh PTD solutions and PTD solutions aged for about 60 days.

This project has received funding from the EURATOM research and training programme 2014-2018 under grant agreement No 755171. The content of this deliverable reflects only the author's view. The European Commission is not responsible for any use that may be made of the information it contains.

Solutions were diluted by $1x10^4$ in 50/50 ACN/H_2O before analysis. The spectra are shown in Figure 34. Both solutions consisted of 0.08M PTD in 0.44M HNO_3. The primary peak was the PTDH+ adduct at 330 m/z. There was a Zn contamination at 361m/z, most likely from the nitric acid stock solution. Contaminants at 312, 302, 270, and 211 m/z were detected in both fresh and aged spectra as well. No significant differences were seen in the two spectra, suggesting that PTD does not undergo degradation in the time frame tested.

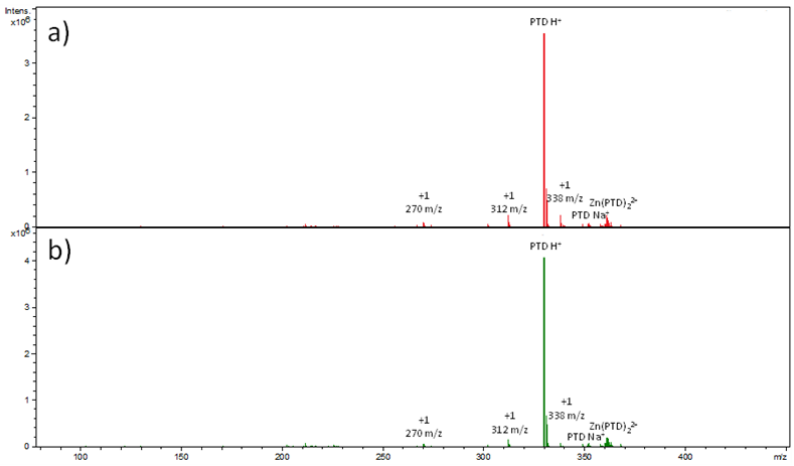

Figure 34: ESI-MS spectra of a) fresh PTD and b) aged PTD (60 days).

ANALYSIS OF GAMMA IRRADIATED PTD SOLUTIONS

Then ESI-MS analyses were performed on solutions of PTD (0.08M PTD, 0.44M HNO_3) that had been previously irradiated to 100 kGy and 200 kGy by POLIMI. Solutions were diluted by $1x10^4$ in 50/50 ACN/H_2O before analysis. The ESI-MS are shown in Figure 35. Several degradation products were identified. A summary of all the degradation products found and the conditions they were found under is shown in Table 6. The mechanisms of degradation include loss of a side chain, H_2 abstraction, OH addition, and NO_3 addition.

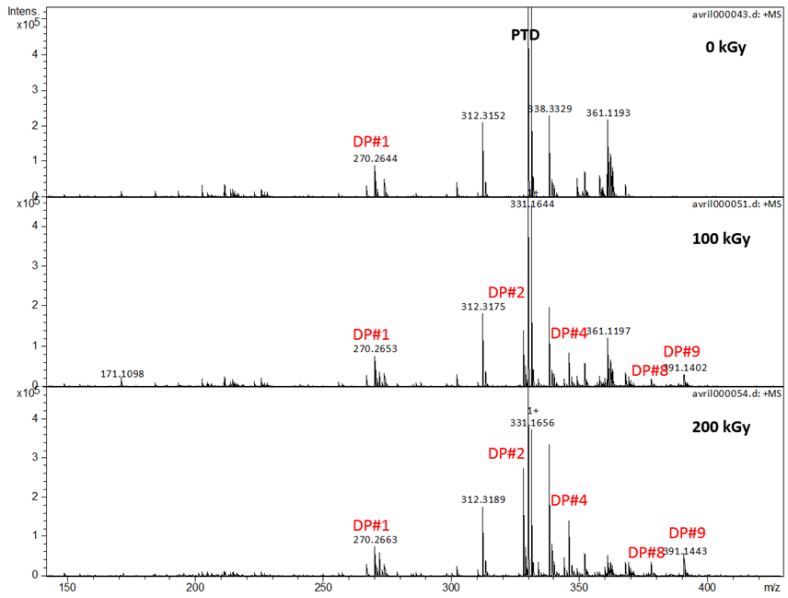

Figure 35: ESI-MS spectra of gamma irradiated PTD solutions: a) fresh PTD solution, b) solution irradiated to 100kGy, c) solution

This project has received funding from the EURATOM research and training programme 2014-2018 under grant agreement No 755171. The content of this deliverable reflects only the author's view. The European Commission is not responsible for any use that may be made of the information it contains.

irradiated to 200kGy. Solutions are 0.08M PTD in 0.44M HNO_3.

ESI-MS analyses of fresh and irradiated PTD solutions that had been used to strip 1mM Am^{3+} from a 0.1M TODGA organic phase were also performed, however the concentration of Am^{3+} was too low to identify any Am^{3+} species. Instead, a solution containing half of the degraded solution and 5mM Am^{3+} was diluted by 10^{-4} in acetonitrile for ESI-MS analysis of the Am^{3+} complexes formed (Figure 36). All degradation products found are listed in Table 6. Most of the degradation product peaks appear after 100kGy of irradiation. The only exception is DP#6, which seems to form a complex with Am in the aged solution as well.

Table 6: PTD degradation products found by ESI-MS analysis, and Am species identified in the mass spectra.

DP	mass	Possible Structure	Radiation Condition	Am^{3+} Complexes
DP#1	271	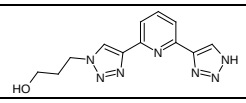	γ >100kGy α >250kGy	None
DP#2	313	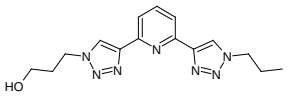	γ >100kGy	$Am(PTD)_2(DP\#2)^{3+}$ $Am(PTD)(DP\#3)(DP\#2)^{3+}$ $Am(DP\#3)_2(DP\#2)^{3+}$
DP#3	327	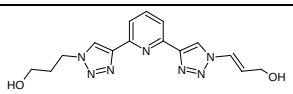	γ >100kGy α >175kGy	$Am(PTD)_{0-2}(DP\#3)_{1-3}^{3+}$ $Am(NO_3)_2(PTD)_{0-1}(DP\#3)_{1-2}^{+}$
DP#4	343	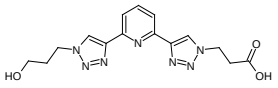	γ >100kGy α >250kGy	$Am(PTD)_2(DP\#4)^{3+}$ $Am(PTD)(DP\#3)(DP\#4)^{3+}$ $Am(DP3)_2(DP\#4)^{3+}$ $Am(NO_3)_2(PTD)(DP\#4)^{+}$ $Am(NO_3)_2(DP\#2)(DP\#4)^{+}$
DP#5	345	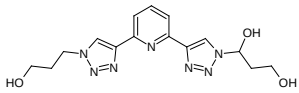	γ >100kGy α >250kGy	$Am(PTD)_2(DP\#5)^{3+}$ $Am(PTD)(DP\#3)(DP\#5)^{3+}$ $Am(NO_3)_2(PTD)(DP\#5)^{+}$ $Am(NO_3)_2(DP\#3)(DP\#5)^{+}$
DP#6	359	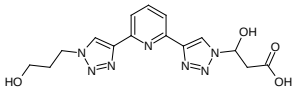	γ >100kGy α >250kGy	$Am(PTD)_2(DP\#6)^{3+}$ $Am(PTD)(DP\#3)\ (DP\#6)^{3+}$ $Am(DP3)_2(DP\#6)^{3+}$ $Am(NO_3)_2(PTD)(DP\#6)^{+}$ $Am(NO_3)_2(DP\#3)(DP\#6)^{+}$
DP#7	374	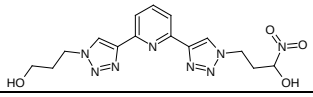	γ >100kGy α >420kGy	$Am(NO_3)_2(PTD)(DP\#7)^{+}$ $Am(NO_3)_2(DP\#3)(DP\#7)^{+}$
DP#8	375	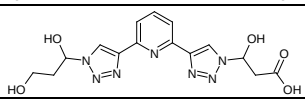	γ >100kGy α >420kGy	$Am(PTD)_2(DP\#8)^{3+}$ $Am(PTD)(DP\#3)(DP\#8)^{3+}$ $Am(DP\#3)_2(DP\#8)^{3+}$
DP#9	377	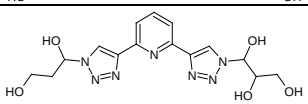	γ >100kGy	None
DP#10	390	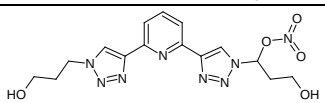	γ >100kGy α >250kGy	$Am(PTD)_2(DP\#10)^{3+}$ $Am(PTD)(DP\#3)(DP\#10)^{3+}$ $Am(DP\#3)_2(DP\#10)^{3+}$ $Am(NO_3)_2(PTD)(DP\#10)^{+`}$ $Am(NO_3)_2(DP\#3)(DP\#10)^{+}$

This project has received funding from the EURATOM research and training programme 2014-2018 under grant agreement No 755171. The content of this deliverable reflects only the author's view. The European Commission is not responsible for any use that may be made of the information it contains.

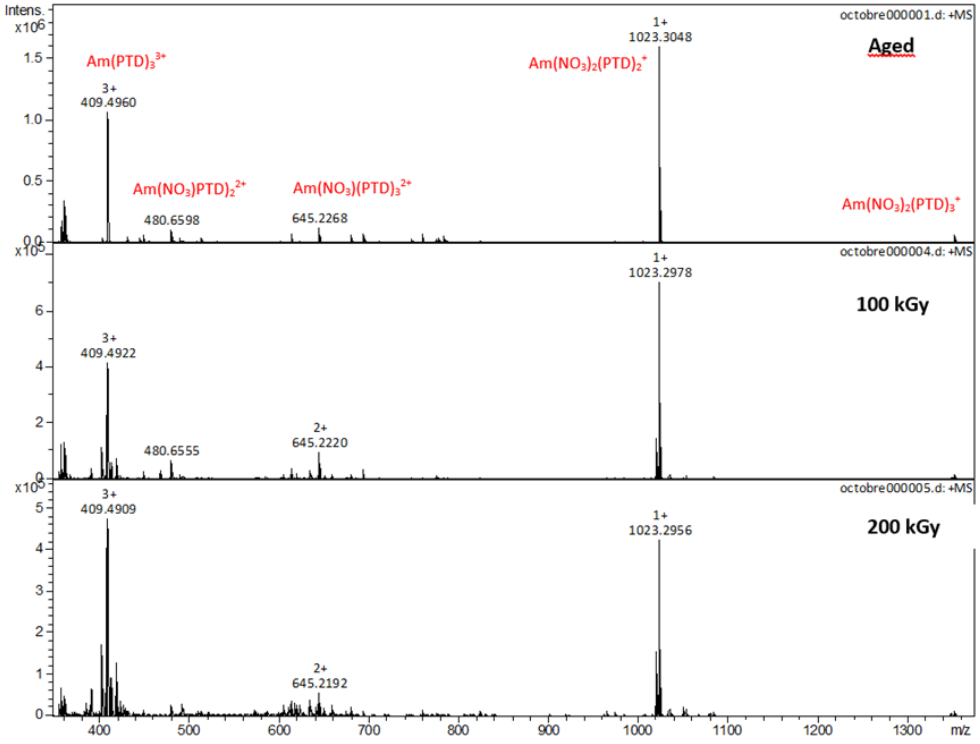

Figure 36: ESI-MS of gamma irradiated PTD solutions (0.08M PTD/ 0.44M HNO_3), diluted by ½ and with 5mM of ^{242}Am added. The main Am-PTD adducts are shown in the top panel (aged PTD).

ANALYSIS OF ALPHA IRRADIATED PTD SOLUTIONS

To determine how alpha irradiation affects the degradation of PTD and to determine which degradation products are likely to complex Am^{3+} in stripping, 10mM of ^{242}Am was added to 0.09M PTD in 0.5M HNO_3. With time, the alpha radiation from with Am will radiolytically degrade the PTD in-situ.[1] ESI-MS spectra were recorded at set intervals to identify the degradation products and Am^{3+} complexes formed in solution. Samples were diluted by $1x10^4$ in ACN prior to ESI analysis. The spectra are shown in Figure 37 and Figure 38. More degradation products were visible in Am adducts than H^+ or Na^+ adducts, showing a strong affinity of these compounds for Am^{3+} (Table 6).

As with gamma irradiation, most of the products appear to be the result of H_2 abstraction, OH addition, and NO_3 addition. Products with two oxygen additions and NO_2 additions also appear at higher doses (Table 6). The Am^{3+}

[1] ^{241}Am was added to the solutions as follows: 10µL of a 0.034M ^{241}Am solution was diluted into 35µL of 0.1M HNO_3 to create a 10mM solution of Am. 10µL of this Am solution was then added to 10 µL of each PTD solution (initial [PTD] = 0.08M, 0.44M HNO_3) and this was diluted to 1mL using ACN. The resulting solution was diluted by another factor of 100 in ACN for ESI-MS analysis. The alpha irradiation solution was prepared as follows: 90µL of 0.09M PTD was prepared in 0.44M HNO_3, then a 10 µL spike of 0.1 M Am^{3+} in 3M HNO_3 was added, bringing the HNO_3 concentration to 0.5M. The solution was left to irradiate in a glovebox, with 10µL samples removed and diluted by 10^4 in acetonitrile every few days for ESI-MS analysis.

This project has received funding from the EURATOM research and training programme 2014-2018 under grant agreement No 755171. The content of this deliverable reflects only the author's view. The European Commission is not responsible for any use that may be made of the information it contains.

complexes shown are also best guesses based on the mass of the complex and the isotopic pattern. There are several ways that several of Am^{3+} masses could be accounted for, i.e. both $Am(DP\#2)_2(DP\#6)^{3+}$ and $Am(PTD)(DP\#2)(DP\#7)^{3+}$ would appear at 412.8 m/z. In this report, usually the simplest possible complex is written for each mass.

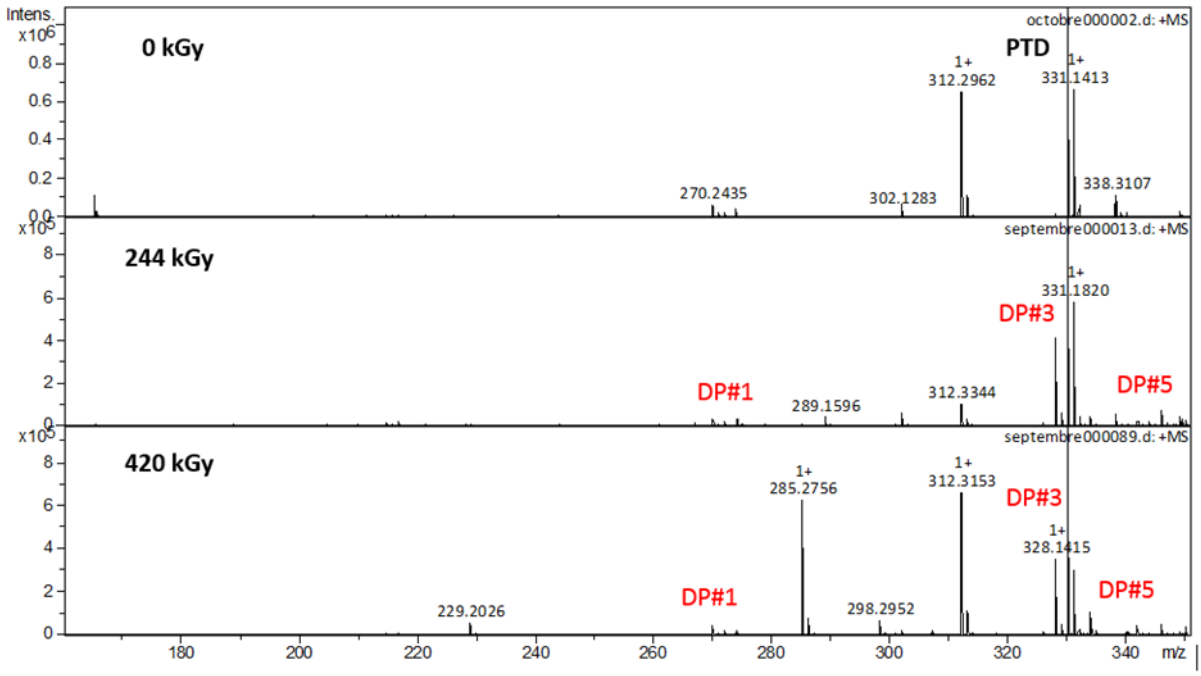

Figure 37: ESI-MS spectra (160-350 m/z) of in-situ alpha irradiated PTD solutions (0.08M PTD, 0.5M HNO_3).

The most consistent degradation product formed throughout this analysis is DP3, or the removal of H_2 from the PTD molecule. DP3 appears in all irradiated samples and is significant in all of the Am^{3+} adduct peak formations. It is the only degradation product that appears alongside another degradation product in an Am^{3+} complex (i.e. as $Am(NO_3)_2(DP3)(DP6)$). The exact location of the H_2 abstraction on the PTD molecule is currently unknown. Based on the fragmentation spectra, a degradation schema for PTD is proposed in Figure 39. The exact location of the radical additions and the mechanisms of formation are still under debate.

This project has received funding from the EURATOM research and training programme 2014-2018 under grant agreement No 755171. The content of this deliverable reflects only the author's view. The European Commission is not responsible for any use that may be made of the information it contains.

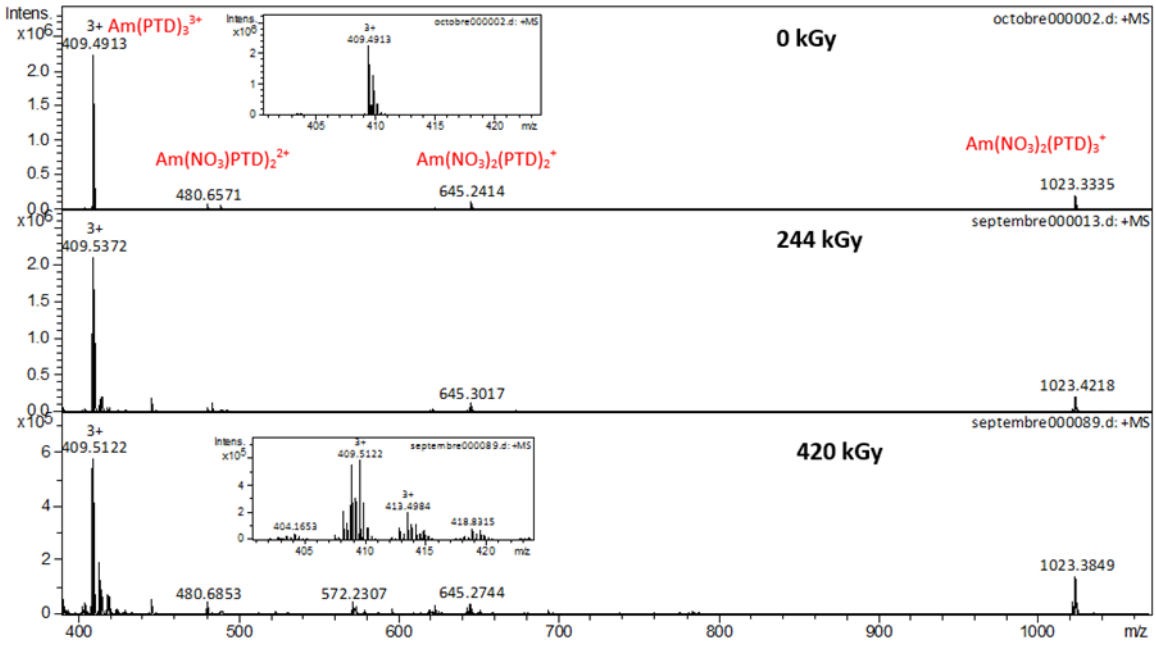

Figure 38: ESI-MS spectra (400-1100 m/z) of in-situ alpha irradiated PTD solutions (0.08M PTD, 0.5M HNO_3). Depicted are the major Am^{3+} adducts present in solutions. Insert is a zoom in the 400-425 m/z showing the appearance of $Am(L)_3^{3+}$ species in the irradiated sample.

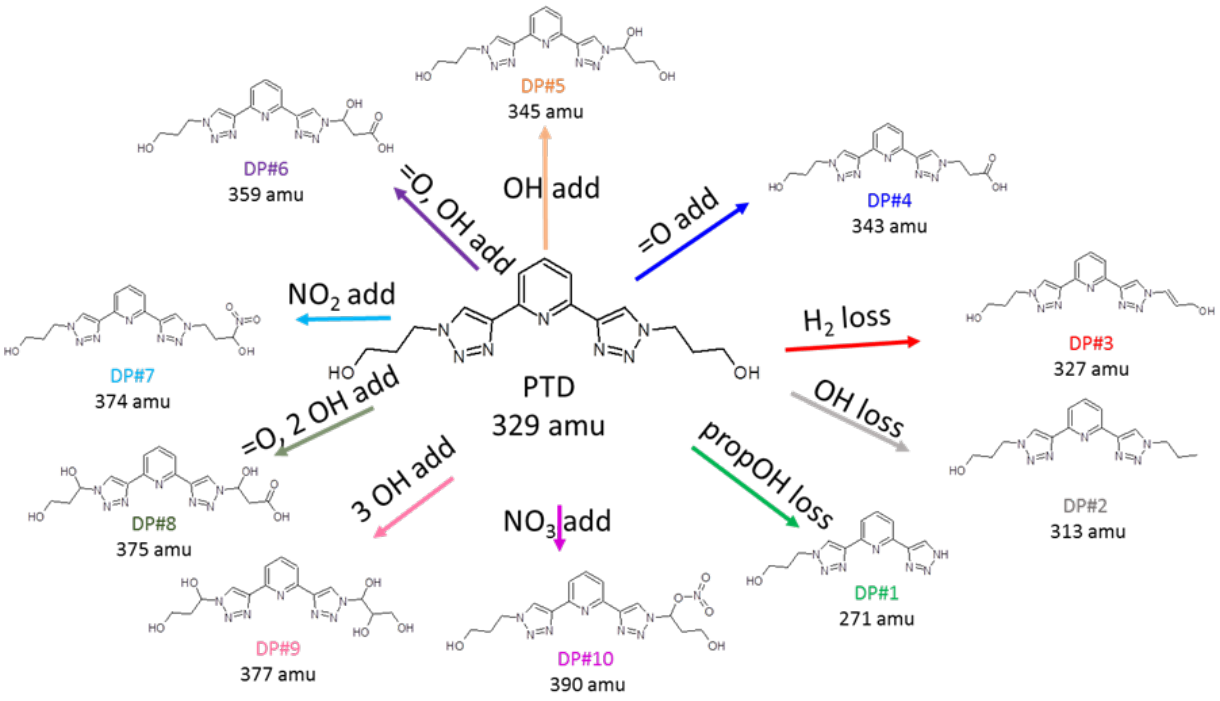

Figure 39: Proposition of a degradation schema for PTD ligand after radiolysis in presence of nitric acid.

This project has received funding from the EURATOM research and training programme 2014-2018 under grant agreement No 755171. The content of this deliverable reflects only the author's view. The European Commission is not responsible for any use that may be made of the information it contains.

FUKUI FUNCTION CALCULATIONS OF PTD

Fukui functions for PTD were calculated to assist in determining degradation product structures. These functions can be used to determine likely sites for electrophilic, nucleophilic, or radical attack on a molecule. The Fukui function used is comprised to three separate equations, listed as follows:

1) $E(A) = P(A)_{n+1} - P(A)$
2) $N(A) = P(A) - P(A)_{n-1}$
3) $R(A) = \frac{1}{2}(P(A)_{n+1} - P(A)_{n-1}) = \frac{1}{2}(E(A) + N(A))$

Where P(A) is the electron population of atom A, $P(A)_{n+1}$ and $P(A)_{n-1}$ are the population around atom A with one atom added or removed from the overall structure, and E(A), N(A), and R(A) are the electrophilic, nucleophilic, and radical Fukui functions respectively.

All calculations were performed using Gaussian 16. Geometry was first optimized for the neutral PTD molecule in the gas phase using the 6-311G basis set. Then a further optimization was done using a CPCM model for water solvation. A final optimization using the 6-311G++(d,p) basis set was then performed. A single point energy calculation was done for the N+1 and N-1 ions of the molecular system, retaining the optimized geometry of the neutral molecule. Calculations were performed on several stereo-configurations of a single PTD molecule, a singly protonated PTD molecule, and a PTD molecule hydrogen bonded to 1 water molecule in 3 different locations. For simplicities sake, only one stereoisomer of each is shown. The results are shown in Figure 40.

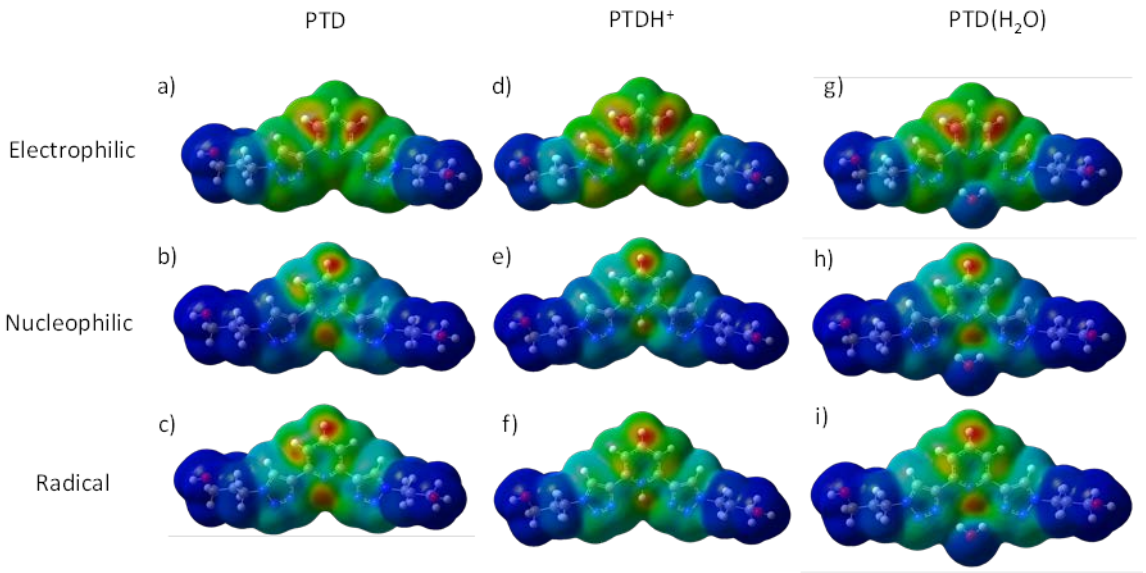

Figure 40: Fukui Function calculation results for PTD. a) Electrophilic function for PTD, b) Nucleophilic function for PTD, c) Radical function for PTD, d) Electrophilic function for $PTDH^+$, e) Nucleophilic function for $PTDH^+$, f) Radical function for $PTDH^+$, g) Electrophilic function for $PTD(H_2O)$, e) Nucleophilic function for $PTD(H_2O)$, f) Radical function for $PTD(H_2O)$.

Most of the attack sites on PTD are located on the pyridine ring with electrophilic attacks preferring the meta positions on the pyridine ring and nucleophilic attacks preferring the pyridine nitrogen and the para position. The radical Fukui function is essentially an addition of the other two functions. Protonating the PTD (pKa = 2.1 [39]) alters the electronic structure of PTD somewhat. The pyridine nitrogen becomes very unlikely to be attacked. The C=C on the triazolyl becomes more susceptible to electrophilic attack as well.

This project has received funding from the EURATOM research and training programme 2014-2018 under grant agreement No 755171. The content of this deliverable reflects only the author's view. The European Commission is not responsible for any use that may be made of the information it contains.

The CPCM model used for solvation does not consider hydrogen bonding, so several calculations were performed with a single water molecule hydrogen bonded to PTD. Oddly, water directly hydrogen bonded to the PTD molecule does not alter the radical attack sites. This hold true even when the water is bonded to the hydroxyl or to only one triazolyl as well (not shown). It could be that it would take multiple water molecules to affect the PTD (which would be time consuming to calculate with this method) or it could be that hydrogen bonds do not affect the electronic structure of PTD enough to change attack sites.

These DFT calculation results are not in good agreement with the experimental results (ESI-MS analysis presented before). Additional calculations that include more explicitly the hydration, the complexation of nitric acid or Am^{3+} would be necessary in order to become significantly helpful in the determination of the PTD degradation scheme.

SYNTHESIS OF PTD DEGRADATION PRODUCTS

UNIPR: A. Casnati, M. C. Gullo, F. Sansone, L. Baldini

The work done in collaboration between UNIPR, POLIMI and CEA showed that upon radiolysis of PTD a certain number of by-products forms. These compounds were separated by HPLC and characterized only by MS spectroscopy, so that only their molecular masses are known but no certainty is present on their molecular structures. Several hypotheses on their structures were proposed but clearly many isomers with the same mass might be equally suggested. For instance, degradation product **DP#6**, whose structure is proposed in Figure 41, might have at least other 9 different isomers (see Figure 41) equally probable. Similarly, compounds due to the reaction with nitric acid such as **DP#7** might also have other 5 different isomers (Figure 42).
Fukui function studies were carried out at CEA supporting the structure of some of these degradation products, but only the isolation of a reasonable (5-10 mg) amount of such compounds and their structural determination will remove all the doubts on their structure. Since the isolation of these quantities from irradiated PTD by preparative HPLC seems to be troublesome due to the complexity of the degradation mixture and scarceness of each component in the mixture, as a synthetic unit we decided to tackle the problem in a different way. We planned to synthesise some of the most plausible compounds and to verify their presence in the irradiated mixture by HPLC analysis. Also MS/MS experiments (comparison of the MS spectra obtained by isolation of a selected molecular ion and observation of its fragmentation upon collision-induced dissociation) will hopefully help in the structure determination of degradation products.

Most of these degradation products lost the C2v symmetry of the starting PTD ligand due to a single reaction on only one of the two arms or two reactions in two different positions of the two arms. The most relevant problem of the synthesis of these degradation products is therefore connected to the differentiation of the two arms connected to the pyridine nuclei especially because this differentiation has to take likely place in the stage of Huisgen cycloaddition reaction. This reaction is known as “click reaction” meaning that is extremely fast and therefore it resulted to be not easy to differentiate the reactivity of the two alkyne arms.

This project has received funding from the EURATOM research and training programme 2014-2018 under grant agreement No 755171. The content of this deliverable reflects only the author’s view. The European Commission is not responsible for any use that may be made of the information it contains.

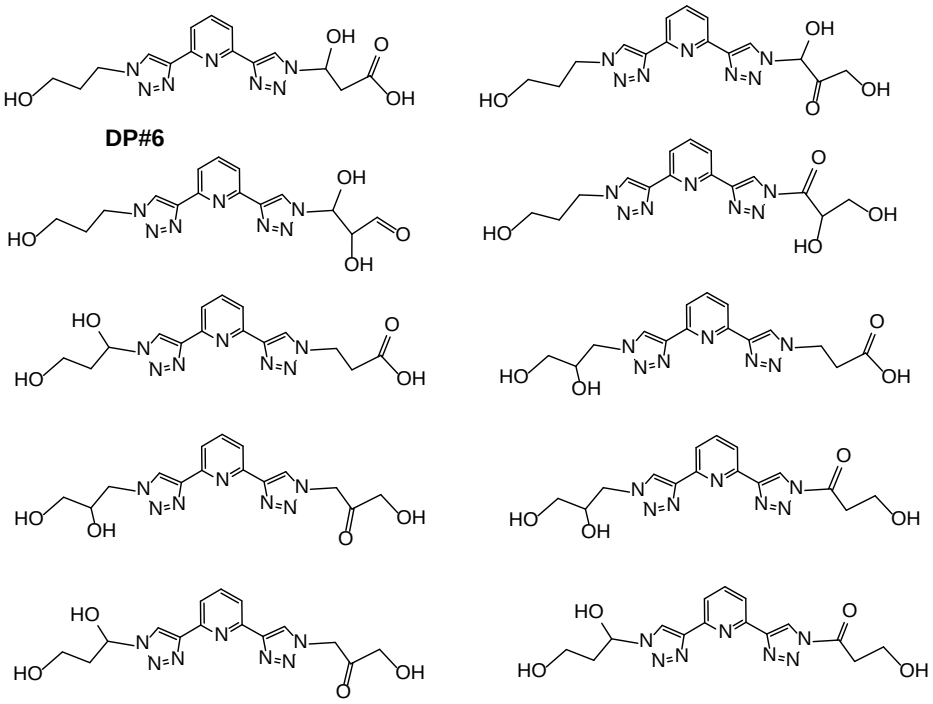

Figure 41: Possible structural isomers of DP#6 (m/z = 359 amu).

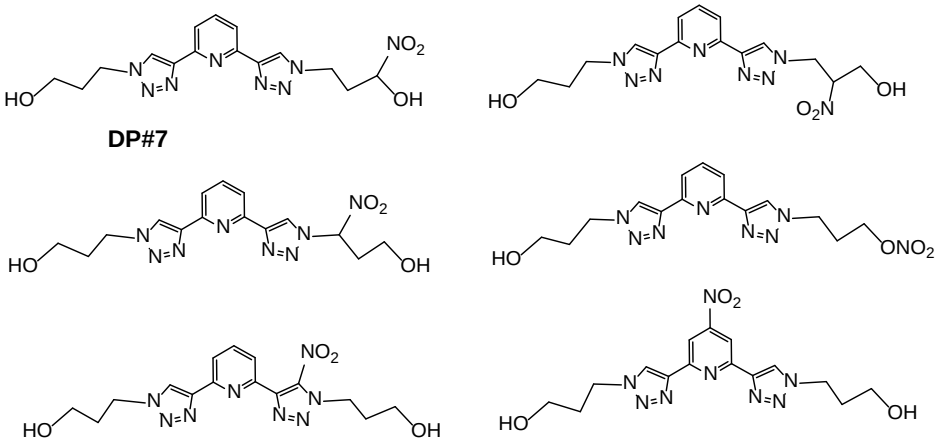

Figure 42: Possible structural isomers of DP#7 (m/z = 374 amu).

First of all, we decided to first try the syntheses of compounds **DP#1** and **DP#4**. Since they are the results of a single modification in the structure of PTD, they should be more abundant. **DP#1** has no other possibility of isomerism. **DP#4** (see Figure 43) has "only" three other possible isomers and, since it should be the father of other degradation products, the disclosure of its structure could help in the determination of the structure of other compounds.

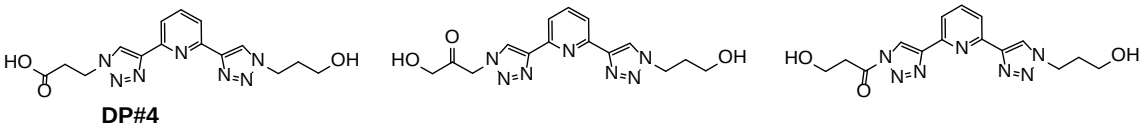

Figure 43: Possible structural isomers of DP#4 (m/z = 343 amu).

This project has received funding from the EURATOM research and training programme 2014-2018 under grant agreement No 755171. The content of this deliverable reflects only the author's view. The European Commission is not responsible for any use that may be made of the information it contains.

We therefore prepared the 3-azido-propanol and ethyl-3-azido propanoate by direct substitution of the halogen atom into commercially available 3-chloropropanol and ethyl-3-bromopropanoate, respectively (Figure 44).

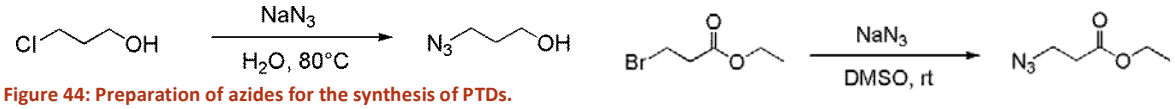

Figure 44: Preparation of azides for the synthesis of PTDs.

For the synthesis of compound **4**, precursor of **DP#4** (**6** in Figure 45), we first tried a direct statistical approach, reacting the starting 2,6-diethynyl pyridine with 1 equivalent of ethyl 3-azido-propanoate and 1 equivalent of 3-azido-propanol under Huisgen cycloaddition conditions. Unfortunately, the ethyl-3-azido-propanoate revealed to be less reactive than 3-azido-propanol and we could only recover PTD and unreacted 2,6-diethynyl-pyridine.

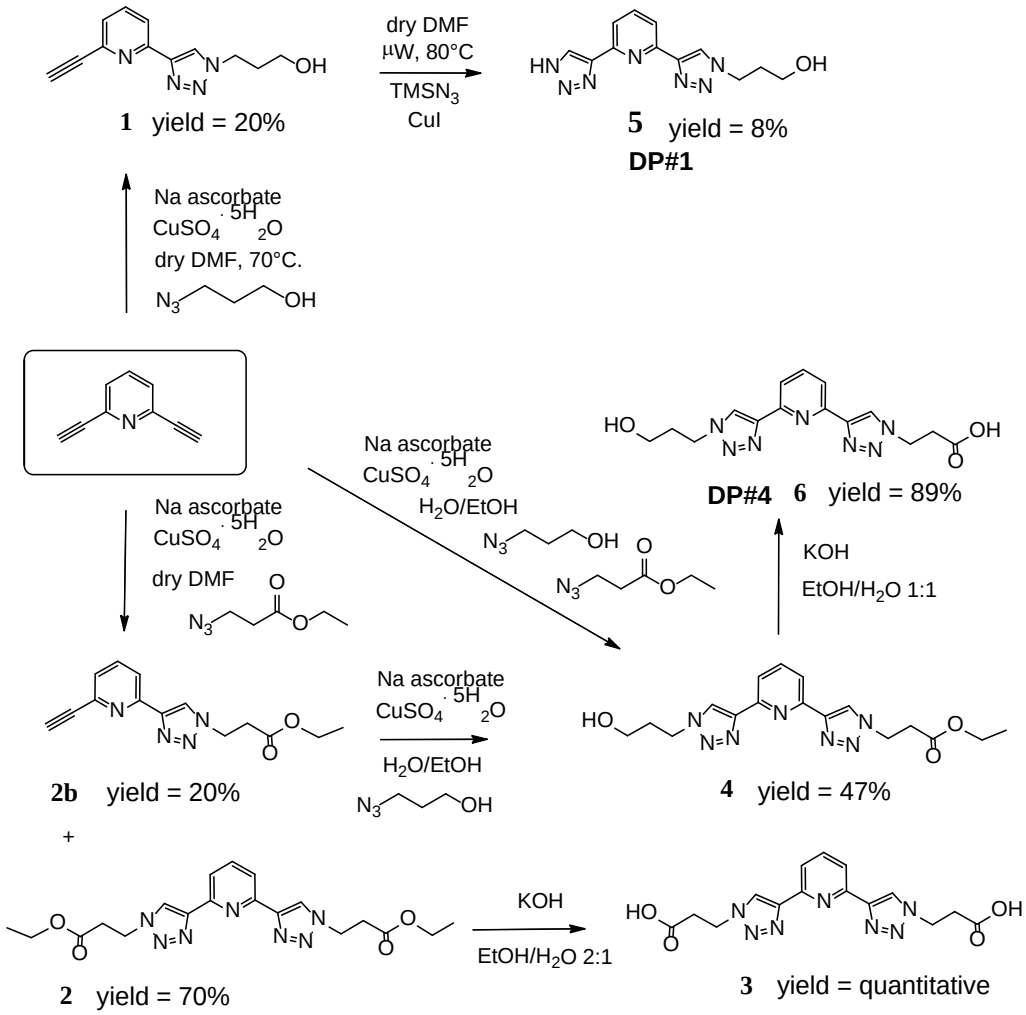

Figure 45: Scheme of the synthesis of possible degradation products.

We consequently tried to study the selective cycloaddition reaction with 3-azidopropanol to obtain compound **1** (Figure 45), but the reaction again seems to be not so selective. Even in the presence of 1 equivalent (or even less) of azide, the main product is PTD which could be recovered with starting material and only a small amount of the desired monofunctionalised compound **1**. Conditions were however developed to allow a 20% formation

This project has received funding from the EURATOM research and training programme 2014-2018 under grant agreement No 755171. The content of this deliverable reflects only the author's view. The European Commission is not responsible for any use that may be made of the information it contains.

of **1**, which could be chromatographically separated from PTD on silica gel. Compound **1**, although obtained in low yields, represents an important intermediate because from this molecule it would be possible to prepare, upon cycloaddition with the appropriate azide, all the degradation products of PTD having an altered propanol arm.

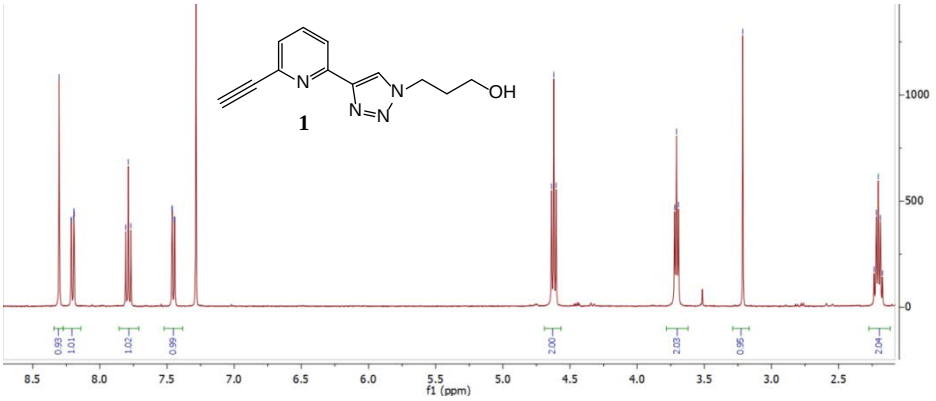

Figure 46: ^{1}HNMR spectrum ($CDCl_3$, 400 MHz, 300K) of compound 1.

The identity of this compound was verified by MS spectroscopy, showing the proper m/z value, and by its ^{1}HNMR spectrum which shows the presence of the ethynyl proton at 3.21 ppm and of a single signal (integrating 1H) at 8.30 ppm for the triazole (CH) proton. Although not identified as a degradation product, Compound 1 was in any case sent to POLIMI to verify its presence in the irradiated PTD mixture (its presence could be justified by a retro-Huisgen reaction).

Reaction of **1** with trimethylsilyl azide (TMSN3) in a microwave oven allowed to obtain, although in quite low yields (8%) compound **5**, identified by POLIMI and CEA as **DP#1**. Its ^{1}HNMR spectrum (Figure 47) confirms the loss of symmetry compared to PTD and the appearance of two different signals for the CH triazol groups at 8.66 and 8.47 ppm for the unfunctionalised and functionalised triazole units, respectively.

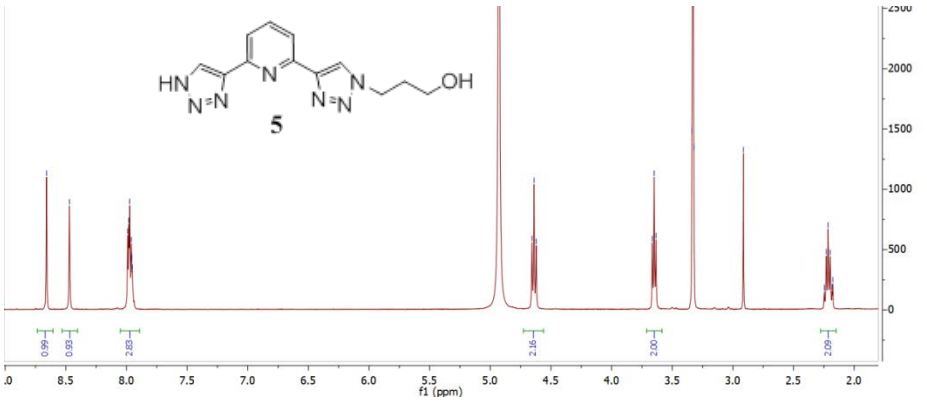

Figure 47: ^{1}HNMR spectrum (CD_3OD, 400 MHz, 300K) of compound 5.

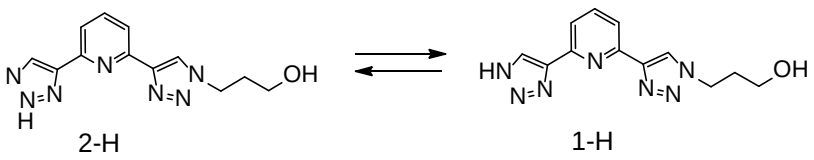

Figure 48: Tautomerism between 1-H and 2-H forms of 1,2,3-triazole in compound 5

This project has received funding from the EURATOM research and training programme 2014-2018 under grant agreement No 755171. The content of this deliverable reflects only the author's view. The European Commission is not responsible for any use that may be made of the information it contains.

It has to be noted that, as reported in the literature [41,42], a tautomerism between the two forms 1-H and 2-H of 1,2,3-triazole is effective in water and protic solvents with a slight preference (2/1) for the 2-H form (Figure 48).

For the synthesis of compound **6** (**DP#4**) it was followed a different synthetic route. First, it was introduced the oxidized arm bearing the carboxy group. The 2,6-diethynyl pyridine was in fact reacted with ethyl 3-azidopropanoate in the presence of copper sulfate and ascorbic acid. The reaction was stirred without heating (room temperature) for 24 hs in order to favour the product of monofunctionalisation 2b upon the difunctionalised compound **2**. After quenching and purification, the two compounds were isolated in 20% and 70% yields, respectively. Compound **2b** was subsequently reacted under Huisgen cycloaddition conditions with 3-chloropropanol to obtain compound **4** (yield = 47%) and subsequently hydrolyzed under basic conditions to afford compound **6** (**DP#4**) in 89% yield.

In parallel, also compound **2** was hydrolyzed in basic conditions and the diacid **3** was obtained quantitatively. Figure 49 shows the ^{1}HNMR spectrum of compound **3**.

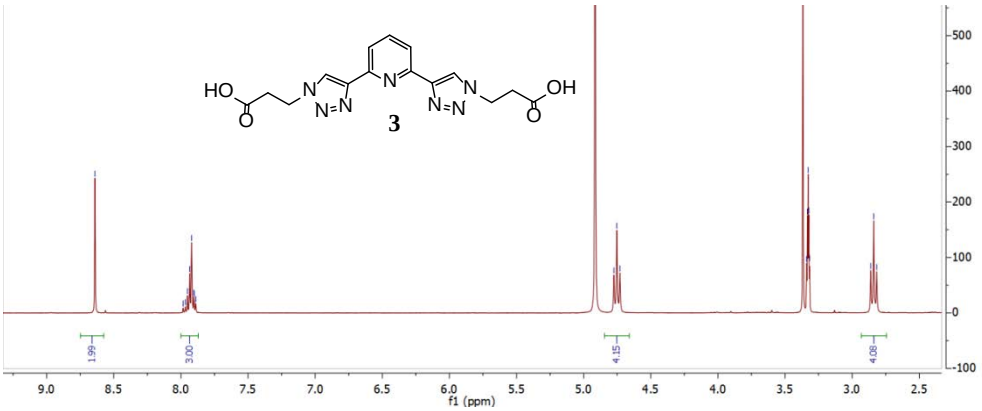

Figure 49: ^{1}HNMR spectrum (CD_3OD, 300 MHz, 300K) of compound 3.

Compounds **1**, **5**, **3** and **6** were sent to POLIMI in order to verify their presence in the irradiated PTD solution.

CONCLUSIONS

The studies performed by POLIMI enabled to assess that ageing up to 341 days of the PTD-based stripping solvent, as well as gamma irradiation up to 200 kGy at 2.5 kGy h^{-1}, does not lead to a worsening of the extracting performances. Even the PTD loading capability under *i*-SANEX conditions is kept unaltered in aged and irradiated (up to 200 kGy) PTD solutions. Instead, it was observed that an absorbed dose of 500 kGy degrades the PTD capability to separate Am from Eu. Furthermore, experiments revealed that pre-equilibrium of the aqueous stripping phases with the TODGA-based organic phase has no effect before ageing, while it could lead to a slight decrease of the Eu distribution ratio and thus of the separation factor before gamma irradiation.
From a qualitative point of view, the present studies demonstrated that ageing (after 60 days up to 340 days) and hydrolysis in nitric acid solutions (0.44 and 5 M HNO_3) has no (or insignificant) effect on PTD: no degradation products were detected. Studies performed by POLIMI and CEA led to coherent conclusions.
Concerning the radiolytic degradation, the effect of gamma irradiation on PTD solutions was extensively studied by means of HPLC-ESI-MS and tandem mass spectrometry at POLIMI. Several degradation by-products were observed and some possible molecular structures were hypothesized on the basis of radiation chemistry literature and the mass tandem spectrometry experiments. Consequently, to the most probable reaction of

This project has received funding from the EURATOM research and training programme 2014-2018 under grant agreement No 755171. The content of this deliverable reflects only the author's view. The European Commission is not responsible for any use that may be made of the information it contains.

hydrogen atom abstraction from the C-H bond in alpha position with respect to the triazolyl ring or to the alcoholic group, the proposed degradation paths entail the addition of radical species coming from diluent radiolysis. On the other hand, the branch loss could follow hydrogen atom abstraction from the alpha position adjacent to the triazolyl ring. Furthermore, the proposed PTD by-products structures, all preserving the complexing core, are compatible with the liquid-liquid extraction results obtained. The ligand concentration reduction was evaluated highlighting a dose rate effect: a similar decrease was obtained at 100 kGy at the lower dose rate of 0.13 kGy h^{-1} and at 200 kGy at the higher dose rate of 2.5 kGy h^{-1}. Similarly, a semi-quantitative analysis of the by-products concentration was attempted.

Gamma and alpha irradiations of similar PTD solutions lead to the formation of similar degradation products of PTD, with a minor impact on the PTD complexation site. The main benefit of performing alpha irradiation experiments is to get easier access and better identification of the degradation product complexes with Am^{3+}. The DFT & Fukui calculations performed here were not satisfactory: this method is not entirely suitable in the aqueous phase, where solvation and environment effects (and complexation of Am^{3+}), that play an important role, would have to be taken into account more explicitly. However, the experimental results allowed us to propose a degradation schema for the PTD complexing agent.

On the basis of the work done by POLIMI and CEA, UNIPR selected some degradation products and succeeded in their synthesis. They will be used as standard compounds to confirm the identity of the degradation products present in the irradiated PTD solutions and to enable a quantitative analysis.

DISTRIBUTION RATIO OF Eu(III) AND Am(III) AS A FUNCTION OF CONTACT TIME FOR BOTH PTD OR SO_3PhBTP

CNRS-Phenix: T. H. Vu and J.-P. Simonin

Aim of this piece of work was to study how do efficiency and selectivity of Am and Eu vary upon long contact times (up to 18 days).

EXPERIMENTAL SECTION

PTD and SO_3PhBTP were kindly provided to us by Alessandro Casnati and Andreas Geist, respectively.

An aqueous nitric acid solution containing the ligand was spiked with the radiotracer Eu-152 or Am-241. It was put in contact with a 0.2 M TODGA (+ 5% vol. 1-octanol) solution in TPH. The volumes of the phases were 0.5 mL each.

The initial value of *D* was measured first. This was done by mixing the two phases during 1 hour and then centrifuging them during 10 min. A 0.3 mL aliquot of each phase was taken and their activity was measured. Samples from the bottom solution were taken carefully in order to not contaminate the sample with traces of the top solution, especially when the latter was much more active than the former (case of high *D*).

After the measurement, the two aliquots were put back into the tube and the solutions were left *in contact* without stirring.

This project has received funding from the EURATOM research and training programme 2014-2018 under grant agreement No 755171. The content of this deliverable reflects only the author's view. The European Commission is not responsible for any use that may be made of the information it contains.

After some time (one or a few days), the two phases were stirred again during 40 min, they were centrifuged and the activity of two samples was measured. Then the latter were introduced back into the tube and the same procedure was repeated in the next measurement.

D AS A FUNCTION OF PTD CONCENTRATION

In Figure 50 it is plotted the variation of the distribution ratio of Eu-152 in the case of 0.5 M nitric acid solutions of different concentrations of PTD ligand (from 40 mM to 100 mM). As can be seen, for all studied PTD concentrations, *D* was found to increase considerably during the first 4 days, after which it somewhat decreased. The *D* values after 10 days and 17 days seem stable, but higher than the initial value (at *t*= 0).

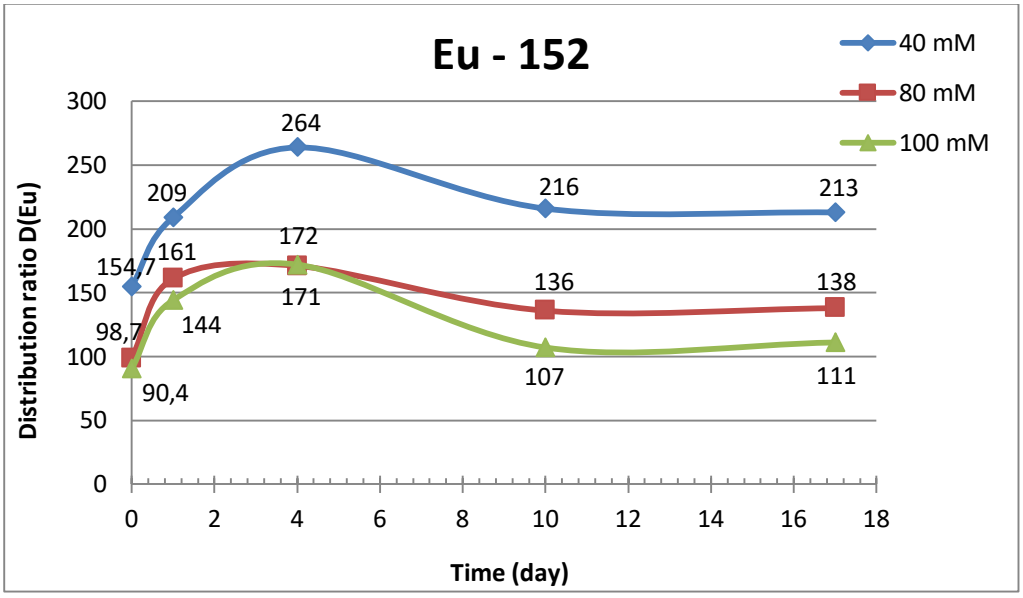

Figure 50: Distribution ratio of Eu-152 measured as a function of time. Organic phase: 0.2M TODGA (+ 5% vol. octanol-1) in HTP. Aqueous phase: various [PTD] in 0.5 M HNO_3 solutions.

The variation of *D* with time for Am-241 is plotted in Figure 51. At all studied PTD concentrations, *D* was observed to increase considerably during the first 11 days, and then to decrease until *t* =18 days.

This project has received funding from the EURATOM research and training programme 2014-2018 under grant agreement No 755171. The content of this deliverable reflects only the author's view. The European Commission is not responsible for any use that may be made of the information it contains.

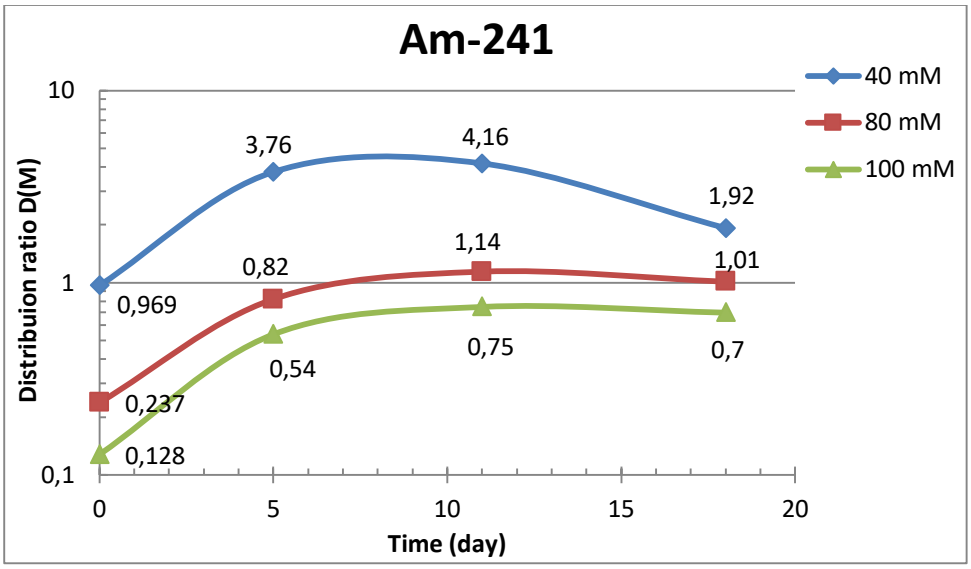

Figure 51: Distribution ratio of Am-241 measured as a function of time. Organic phase: 0.2 M TODGA (+ 5% vol. octanol-1) in HTP. Aqueous phase: various PTD concentrations in 0.5 M HNO_3 solutions.

In another type of experiment, *D* was monitored with time when the 2 phases were kept separately after the initial measurement, as was done by POLIMI. We obtained the same result as POLIMI (as reported in HYPAR-1), namely that *D* does not vary with time when the two phases are *not* in contact.

D AS A FUNCTION OF NITRIC ACID CONCENTRATION

In Figure 52 and 54 is plotted the variation of the distribution ratio of Eu-152 and Am-241, respectively, in the case of 80 mM PTD solutions of different concentrations of nitric acid varied from 0.1 M to 0.75 M.

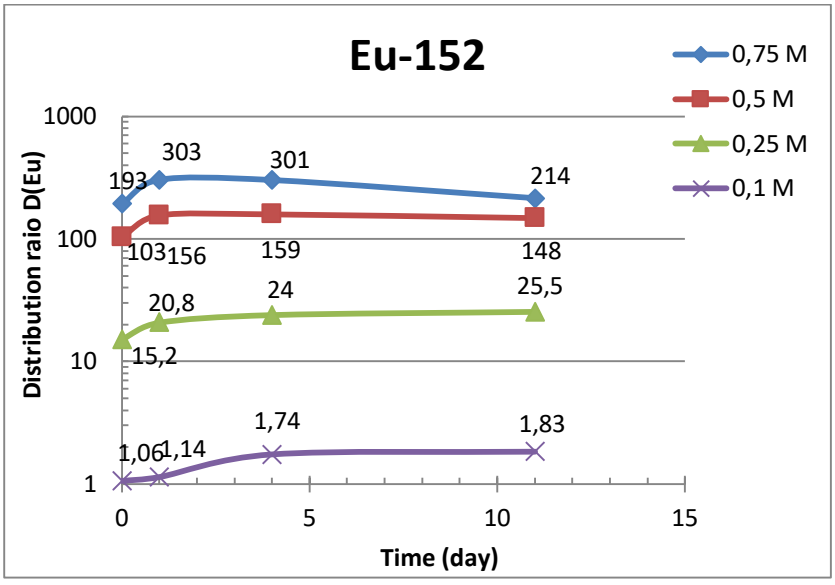

Figure 52: Distribution ratio of Eu-152 measured as a function of time. Organic phase: 0.2 M TODGA (+ 5% vol. octanol-1) in HTP. Aqueous phase: 80 mM PTD in various [HNO_3].

This project has received funding from the EURATOM research and training programme 2014-2018 under grant agreement No 755171. The content of this deliverable reflects only the author's view. The European Commission is not responsible for any use that may be made of the information it contains.

The variation of D/D_0 (with D_0 the value of D at t = 0) as a function of time in the case of Eu(III) is plotted in Figure 53.

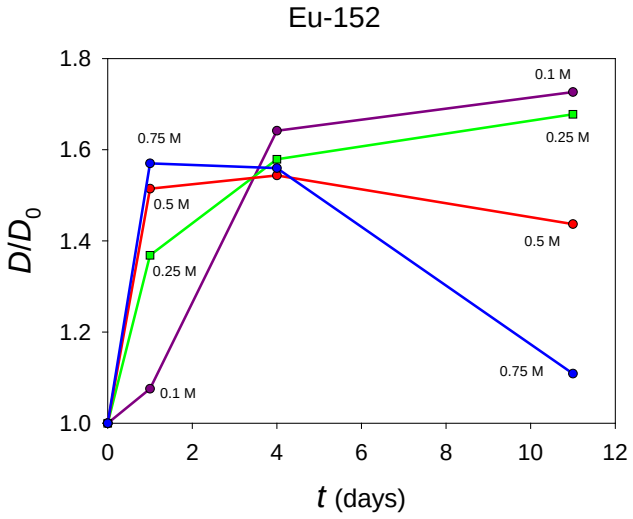

Figure 53: D/D_0 in the case of Eu-152 as a function of time. Organic phase: 0.2 M TODGA (+ 5% vol. octanol-1) in HTP. Aqueous phase: 80 mM PTD in various [HNO_3] (from 0.1 M to 0.75 M).

This figure shows that the relative variation of D exhibits a peculiar variation. After 1 day it is in the order of the acid concentration. This variation seems to be "catalysed" by the presence of HNO_3. On the other hand, the reverse phenomenon is observed for longer times (after 11 days), at which D/D_0 nearly returns to its initial value, which is not the case of the lower nitric acid concentrations.

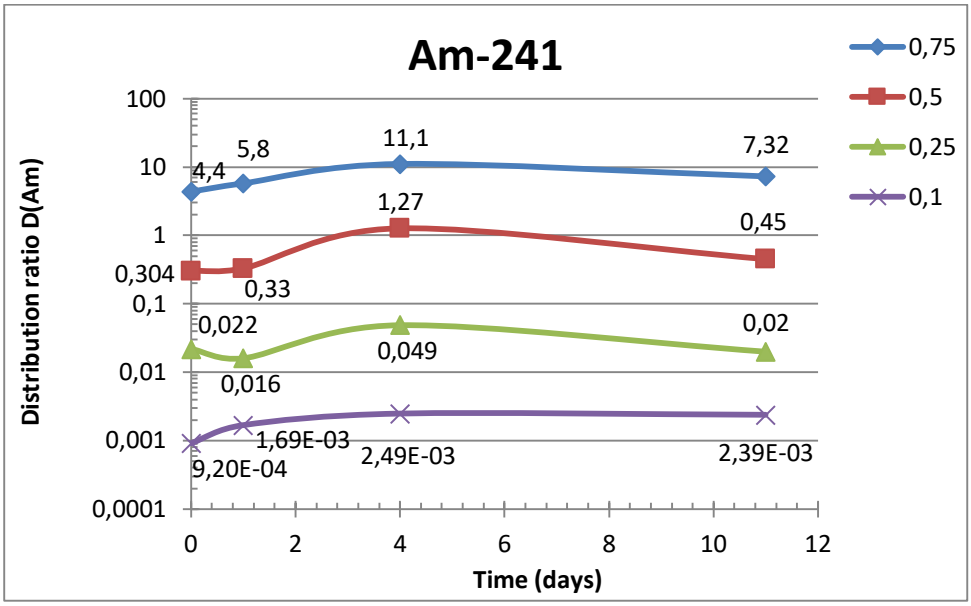

Figure 54: Distribution ratio of Am-241 measured as a function of time. Organic phase: 0.2 M TODGA (+ 5% vol. 1-octanol) in HTP. Aqueous phase: 80 mM PTD with various [HNO_3].

This project has received funding from the EURATOM research and training programme 2014-2018 under grant agreement No 755171. The content of this deliverable reflects only the author's view. The European Commission is not responsible for any use that may be made of the information it contains.

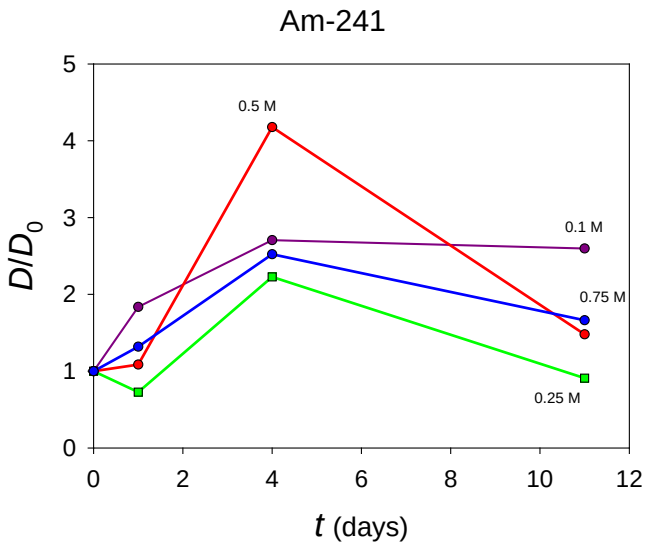

Figure 55: D/D_0 in the case of Am-241 as a function of time. Organic phase: 0.2 M TODGA (+ 5% vol. octanol-1) in HTP. Aqueous phase: 80 mM PTD in various [HNO_3] (from 0.1 M to 0.75 M).

Surprisingly, the variation of D/D_0 in the case of Am(III) is not identical to that of Eu(III). It is not correlated with the amount of nitric acid at short times, nor it is correlated at long times (11 days). The point for 0.5 M HNO_3 is surprisingly high; we did not have time to repeat this measurement.

Nonetheless, as can be seen in Figures 52-55, the variation of *D* with time is appreciable for the two radioelements.

CASE OF SO_3PHBTP

The variation of *D*(Eu-152) with time was also performed in the case of 20 mM SO_3PhBTP in 0.5 M HNO_3 solution. The *D*(Eu) value was initially **27.8** (after 1h stirring), and then it was **67.9** after 1 day, which is more than a twofold increase. The value of *D*(Eu) was not measured for longer times, or other ligand and nitric acid concentrations.

CONCLUSIONS

Our results suggest that the distribution ratio of Eu(III) and Am(III) varies significantly with the contact time of the phases, in the case of PTD and SO_3PhBTP as the hydrophilic ligand in HNO_3 solution.

REFERENCES

1. A. Geist et al. *Solvent Extr. Ion Exch.* **2012,** *30* (5), 433–444.
2. M. J. Carrot et al. *Solvent Extr. Ion Exch.* **2014,** *32* (5), 447–467.
3. M. Carott et al. *Hydrometallurgy*, **2015**, 139–148**.**
4. R. Malmbeck et al. Proceedings of *Internat. Conf. ISEC 2014,* Würzburg, Germany, 7–11 September **2014**.

This project has received funding from the EURATOM research and training programme 2014-2018 under grant agreement No 755171. The content of this deliverable reflects only the author's view. The European Commission is not responsible for any use that may be made of the information it contains.

5. R. Taylor et al, *Procedia Chemistry*, **2016**, 21, 524 – 529.
6. A. Geist et al. *Internat. Conf. GLOBAL 2013,* Salt Lake City, U.S.A., 29/9 – 3/10/**2013**.
7. A. Wilden et al. Progress in Nuclear Energy, **2014**, 72, 107-114
8. H. Galán et al. *Proceedings of Internat. Conf. ISEC 2014,* Würzburg, Germany, 7–11 September **2014**.
9. E. Macerata et. al., "Process safety studies on hydro-BTP and Pytritetraol." D11.5. of SACSESS Project CONTRACT Nº FP7-CP-2012-323282.
10. H. Galán et al. 2nd edition of the Radical Behavior workshop, Würzburg, Germany, 19–20 April **2018**.
11. D. Magnusson et al. *Radiochim. Acta* **2009**, *97*, 497–502.
12. D. Peterman, et al. *Ind. Eng. Chem. Res* 55.39, **2016**, 10427–10435.
13. S. P. Mezyk et al., *Radioanal Nucl Chem*, **2013**, 296, 711–715.
14. B. Mincher *J. Radioanal. Nucl. Chem.*, **2018**, 316,799–804.
15. J.W.T. Spinks, R.J. Woods "An introduction to radiation chemistry". 3rd Ed. Wiley and Sons, **1991**.
16. A. Geist et al. *Solv. Extr. Ion Exch.*, **2012**, 30, 433–444.
17. M. J. Carrot et al. *Solvent Extr. Ion Exch.* **2014,** *32* (5), 447–467.
18. M. Carott et al. *Hydrometallurgy*, **2015**, 139–148**.**
19. R. Malmbeck et al. *Proceedings of Internat. Conf. ISEC 2014,* Würzburg, Germany, 7–11 September **2014**.
20. R. Taylor et al, *Procedia Chemistry*, **2016**, 21, 524 – 529.
21. L. Berthon et at., Sep. Scie. Techn., **2001**, 36, 709–728.
22. H. Galán First SACSESS International Workshop Warsaw, Poland, 22-24 April, **2015**.
23. C. Wagner et al. *Solvent Extr. Ion Exch.* **2016**, *34* (2), 103–113.
24. C. Wagner, et al. *Dalton Trans.* **2015**, *44* (39), 17143–17151.
25. S. Gracia, et al. *Tetrahedron* **2015**, *71* (33), 5321–5336.
26. N. Boubals, et al. *Inorg. Chem.* **2017**, *56* (14), 7861–7869.
27. H. Galán, et al. In *Proc. Internat. Solvent Extr. Conf. (ISEC 2014)*, Würzburg, Germany, 7–11 September, 2014; pp 137–143.
28. D. Magnusson, et al. *Radiochim. Acta* **2009**, *97* (9), 497–502.
29. Y. Sasaki, et al. *Anal. Sci.* **2007**, *23*(6), 727-731. 10.2116/analsci.23.727.
30. G. J. Lumetta, et al. *Solvent Extr. Ion Exch.* **2014**, *32*(4), 333-347. 10.1080/07366299.2014.895638.
31. C. Rostaing et al. *Procedia Chem.* **2012**, *7*, 367-373. 10.1016/j.proche.2012.10.057.
32. S. Lange et al. *Solvent Extr. Ion Exch.* **2017**, *35*(3), 161-173. 10.1080/07366299.2017.1326761.
33. S. A. Ansari et al. *Chem. Rev.* **2012**, *112*(3), 1751-1772. 10.1021/cr200002f.
34. C. A. Zarzana, et al. *Solvent Extr. Ion Exch.* **2015**, *33*(5), 431-447. 10.1080/07366299.2015.1012885.
35. K. M. Roscioli-Johnson, et al. *Solvent Extr. Ion Exch.* **2016**, *34*(5), 439-453. 10.1080/07366299.2016.1212540.
36. H. Galán, et al. *Dalton Trans.* **2015**, *44*(41), 18049-18056. 10.1039/c5dt02484f
37. B. J. Mincher, et al. *Solvent Extr. Ion Exch.* **2013**, *31*(7), 715-730. 10.1080/07366299.2013.815491.
38. B. J. Mincher, et al. *Solvent Extr. Ion Exch.* **2009**, *27*(1), 1-25.
39. E. Macerata, et al., *J. Am. Chem. Soc.* **2016**, *138*, 7232-7235.
40. C. Wagner, et al. *Inorg. Chem.*, **2017**, *56*, 2135–2144.
41. A. Albert, et al., *J. Chem. Soc. Perkin Trans. II*, **1989**, 1903–1905.
42. M. Bellagamba, et al., *Struct. Chem.* **2013**, *24*, 933–943.

This project has received funding from the EURATOM research and training programme 2014-2018 under grant agreement No 755171. The content of this deliverable reflects only the author's view. The European Commission is not responsible for any use that may be made of the information it contains.